"Design of Elliptical Air Holes In Hexagonal Lattice Photonic Crystal Fiber For Liquid Sensing"

A thesis submitted
by

ASHISH KUMAR
2017PEC5125

Under the guidance of
Dr. Ritu Sharma

In partial fulfillment for the award of the degree of
MASTER OF TECHNOLOGY
to the
DEPARTMENT OF ELECTRONICS AND COMMUNICATION ENGINEERING

Electronics & Communication Engineering Department
Malaviya National Institute of Technology, Jaipur
AUGUST 2019

CERTIFICATE

This is to certify that the dissertation report entitled **"Design of Elliptical Air Holes In Hexagonal Lattice Photonic Crystal Fiber For Liquid Sensing"** has been successfully completed and presented by **Ashish Kumar** of Second year, IV semester in partial fulfillment of degree of **Master of Technology** in **Electronics and Communication** during the academic year **2018-2019** to the best of my knowledge and belief that this work has not been submitted elsewhere for the award of any other degree.

The work has been found satisfactorily carried out by him under my guidance and supervision in the department and is approved for submission.

Date:
Place: Jaipur

Dr. Ritu Sharma
Associate Professor
Department of Electronics and
Communication Engineering
Malaviya National Institute of Technology,
Jaipur
India 302017.

DECLARATION

I, **Ashish Kumar**, declare that this Dissertation titled as **"Design of Elliptical Air Holes In Hexagonal Lattice Photonic Crystal Fiber For Liquid Sensing"** and the work presented in it is my own and that, to the best of my knowledge and belief.

I confirm that major portion of the report except the refereed works, contains no material previously published nor present a material which to be substantial extent has been accepted or the award of any other degree by university or other institute of higher learning. Wherever I used data (Theories, results) from other sources, credit has been made to that source by citing them (to the best of my knowledge). Due care has been taken in writing this thesis, errors and omissions are regretted.

Date:
Place: Jaipur

Ashish Kumar
M.Tech
Department of Electronics and
Communication Engineering
Malaviya National Institute of Technology,
Jaipur, India 302017.

Acknowledgments

I would like to thank all people who have helped and inspired me in the research contributing to this thesis. I take this opportunity to express my deep sense of gratitude and respect towards my Supervisor of the dissertation, Dr. Ritu Sharma, Associate Professor, Department of Electronics and Communication Engineering, Malviya National Institute of Technology. I am very much indebted to him for the generosity, expertise, and guidance; I have received from him while working on this project and through- out my studies. Without his support and timely guidance, the completion of my project would have seemed a far-fetched dream. In this respect, I find myself lucky to have her as my Project Supervisor. She has guided me not only with the subject matter but also taught me the proper style and techniques of working.

I express my sincere gratitude to Dr.K.K.Sharma, Professor, Dr. Ravi Kumar Maddila, Associate Professor, Department of Electronics and Communication Engineering, Malviya National Institute of Technology, for all the knowledge they shared with me, without which our research would have been difficult to conclude.

At last but not the least, I am also and always be grateful to my parents and express my deep respect towards them, who always support me and encourage me at each and every step of my career and life besides this project.

Ashish Kumar

Contents

List of Figures

List of Tables

List of Abbreviations

OF	Optical Fiber
PCF	Photonic Crystal Fiber
PBG	Photonic Bragg Grating
η_{eff}	Effective Refractive Index
λ	Wavelength Of Light
$\wedge$	Pitch Of Air-holes
d	Diameter Of Air-holes

Abstract

Photonic crystal fiber has a geometry which is self-possessed microstructured holes of air cladding running lengthways the entire length of the fiber and also the core can either be solid or hollow. Innumerable properties of PCFs have been explored in the literature which includes limitlessly single mode operation, effective mode area, tailorable dispersion, and high birefringence. In Photonic crystal fiber, the control of light basically happens for the reason that the presence of air holes is there and this light guidance can further be boosted by introducing liquid into the hole(air) of the core. If it is desired to use it as a sensor then this new material insertion is useful because there is high interaction of materials and air holes in fiber. The biggest advantage of optical fiber sensor they have a very small size, high sensitivity and also provide greater flexibility which makes them low cost and very efficient solutions for several industries. In my thesis work, a hexagonal geometry has been studied for liquid sensing. The liquid analytes that are to be sensed are ethanol, benzene as they are the most used components in the chemical and biological industries. Firstly, a simple hexagonal structure is studied and η_{eff} and sensitivity of this structure are calculated. Then, the core structure is modified and decagonal, octagonal and hexagonal geometries are constructed in the core with circular holes. Lastly, these circular holes are replaced by elliptical holes and it is simulated with the help of COMSOL Multiphysics software.

The sensitivity obtained is of the order 40-50 % and confinement loss of order E-09 dB/m which shows that these structures can be used for sensing ethanol, water and benzene and are reliable. For benzene, water and ethanol, the hexagonal structure with a core comprised of hexagonal geometry, made up of circular holes (x as major axis), gives the best results. For this geometry, theη_{eff} values are 1.379, 1.317 and 1.313 for benzene, ethanol, and water respectively.

Chapter 1

Introduction

PCF (Photonic Crystal Fiber) is among the furthermost thought-provoking topics in the research area in the field of optics. It consists of a central defect with the periodic planning of air holes that are present along the complete length of the fiber. Light is guided in the PCF by two different methods so accordingly they are classified as: i) index guided PCF and ii) photonic bandgap fiber PBG. PCF has unique properties like high non-linearity, ultra-flattened chromatic dispersion, low confinement loss, small effective area, etc. It can be used in various applications in diverse fields like biomedical, spectroscopy, pulse compression. It includes their capability of usage under unfavorable environmental circumstances such as high voltages, noise, nuclear radiation, and others.[1], [2], [3], [4]

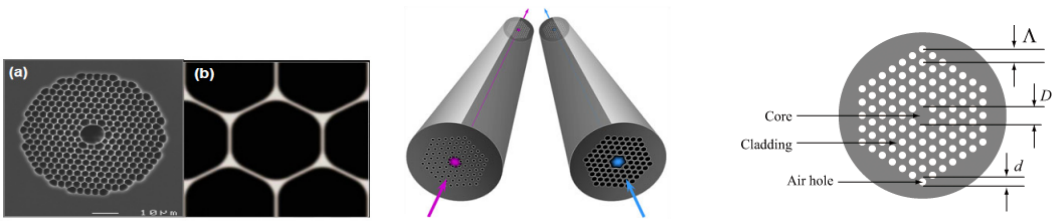

(a) (b) (c)

Figure 1.1: (a) Photonic Crystals (b) Photonic Crystal Fiber (c) Schematic diagram of PCF .

Optical fibers (OFs) were first developed in 1996. They created a revolution in the field of telecommunication and sensing. But in spite of their high performance in the field of telecommunication, there are so many difficulties for the assessment of this technology

due to the intrinsic properties of silica. [1],[2] The evolution of photonic crystal fibers (PCFs) overcome all the problems and limitations related to standard optical fibers. PCF geometry is specified by the presence of air bubbles which are also periodically arranged and are running along the complete fiber length, with either a solid or hollow core in the center.[2] In contrast with standard OF, in PCF we use only one type of material and hence their parameters can be managed easily providing greater adjustability. Additionally, these fibers give the likelihood of light guidance in a hollow core, which unlocks new outlooks in fields such as fiber lasers and fiber sensors.[1]

1.1 Light propagation mechanism in PCF

Light is guided in the PCF by two different methods so accordingly they are classified as:

(i) Index-guided PCF

(ii) Photonic bandgap fiber PBG

1.1.1 Index-guided PCF

Indexed guided PCF operates on the principle of Total Internal reflection (TIR). The cladding comprised of air holes has a refractive index of a lower value as compared to the solid core, so light is guided into the core by reflections at the interface of the less dense medium which befalls when light is made incident at an angle which is larger than the critical angle. Total internal reflection (TIR) is an event which comprises the reflection of all the incident light rays. TIR can only happen when both of the conditions are satisfied by the incident light which is When the light is moving from an optically thicker to an rarer medium and The angle of incidence is greater than critical angle.[1]

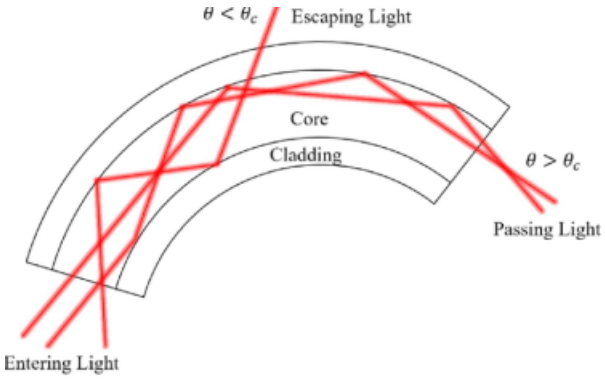

Figure 1.2: Figure showing Total internal reflection in fiber

1.1.2 Photonic bandgap fiber PBG

It occurs in hollow-core PCF in which the periodically distributed air holes of cladding creates a photonic bandgap similar to the electronic bandgap in metals. So, the light is guided into lower refractive index valued core. It is capable of controlling light guidance for any frequency band.

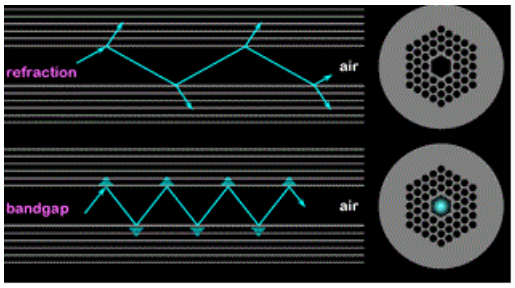

Figure 1.3: Figure showing Index guiding and Photonic bandgap mechanism

1.1.3 Principle of surface plasma resonance

Surface plasmon resonance is a phenomenon in which the coupling of electromagnetic wave and surface plasmon wave is happening on the surface within a metal and a dielectric medium. Surface Plasmon wave is basically a transverse magnetic (TM) polarized EM wave. In SPW the magnetic vector is basically perpendicular to the direction of surface plasmon wave propagation and it is parallel to the plane of the interface. The condition for occurring of SPR when the frequencies and the parallel components of both incident TM polarized EM wave and SPW matched.[1], [5] According to the Maxwell equations

and boundary condition for surface plasmon wave, the propagation constant k_{sp} is given by

$$K_{sp} = \frac{\omega}{c}\sqrt{\frac{\epsilon_m \epsilon_s}{\epsilon_m + \epsilon_s}} \tag{1.1}$$

where ϵ_m is dielectric constant of metal, ϵ_s is the dielectric constant of the dielectric, ω is the frequency of incident light and c is the speed of light.

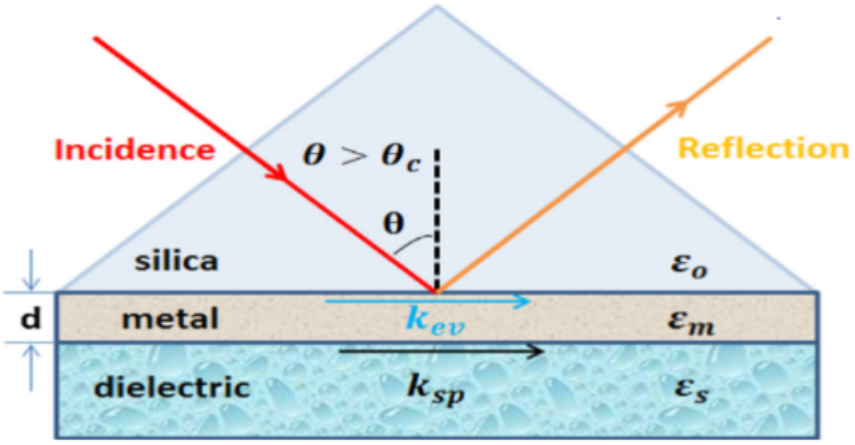

Figure 1.4: Figure showing schematic diagram for surface plasma resonance

Above equation is also appliad to the semi infinite dielectric-metal layers. The propagation constant of the evanescent wave in the direction parallel to the metal surface K_{ev} is given by the following expression:

$$K_{sp} = \frac{\omega}{c}\sqrt{\epsilon_0}\sin\theta \tag{1.2}$$

where ϵ_0 refers to the dielectric constant of the silica in the incidence region. For occurance of SPW only TM polarized wave is required.[2]The surface plasmon resonance occurs only when the wave vector of the evanescent wave matches with that of the surface plasmon wave at a specific angle of incidence. SPR condition is given by:

$$\frac{\omega}{c}\sin\theta_{res} = \frac{\omega}{c}\sqrt{\frac{\epsilon_m \epsilon_s}{\epsilon_0(\epsilon_m + \epsilon_s)}} \tag{1.3}$$

where r_{es} is termed as the resonance angle. This resonance condition also establishes the sensing principle of Surface plasmon resonance sensors. The refractive index of analytes (i.e. $\epsilon_s 1/2$) it can be measured by detecting the resonance angle with a certain incident

wavelength (angle interrogation), or detecting the resonance wavelength with a certain incident angle.[2], [6]

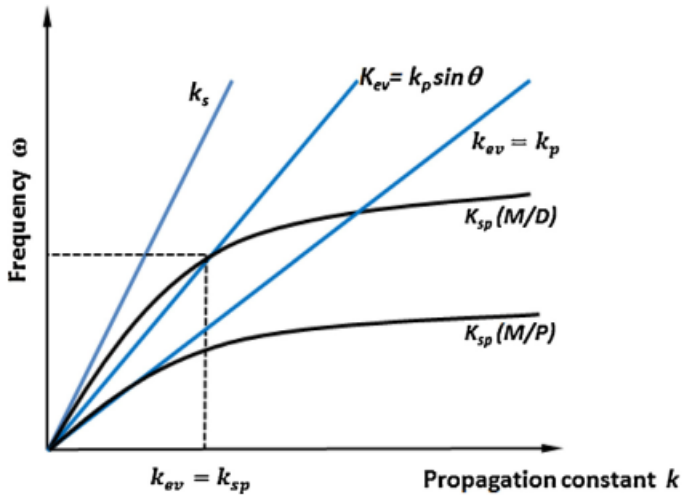

Figure 1.5: Figure showing Incident light wave in dielectric medium (KS), evanescent wave (Kev), the dispersion curve of surface plasma wave of metal-dielectric medium interface (M/D) and metal-prism interface (M/P)

The propagation constant curves of surface plasmon wave and evanescent wave cross at many position between $k_{ev} = k_p \sin$ and $k_{ev} = k_p$ .It indicates that the matching of the evanescent wave and surface plasmon wave depends upon the incident angle and the frequency of source.Another important feature is that the surface plasmon wave on metal–prism interface (M/P) locates on the right of the maximum propagation constant of evanescent wave ($kev = kp$) so that these two curve will never cross. This implies that the surface plasma resonance will never be excited on the metal–prism interface (M/P). [6]

1.2 Sensing application of PCF

The PCF based sensors were first developed in 2000. Since then PCF have found immense growth in this area. PCF has become a very interesting choice for making fiber sensors because it has got various properties which makes it suitable for creating sensors. PCF can be used for creating sensors by varying the size and location of holes in cladding and/or core. The variation in mode shape, birefringence, air filling ratio, non-linearity,

dispersion gives PCF advantages over conventional optical fibers because they can reach values which are not imaginable by the latter. The presence of air hole in core provides a great opportunity of filling it with gas/liquids to check its interaction with the light propagating in the fiber.[2], [6], [4], [7] PCF makes an ideal choice for sensors because of their geometric versatility, greater value of sensitivity over existing technology and their easy compatibility with the existing fiber optical communication systems. The sensors should have certain prominent characteristics which includes flexibility, low cost, small size, high sensitivity, convenient remote monitoring, useable in unfavorable environmental conditions, robustness and multiplexing capability. [8]

1.2.1 Physical sensors

Physical sensors are used for measuring parameters such as temperature, displacement, torsion, pressure, refractive index, electric field, and vibration. The measurement, monitoring, and control of all these parameters are of vast interest for several applications . They are further categorized based on their sensing characteristics.

1.2.2 Displacement/Strain Sensors

The number of applications involve displacement or strain induced change to be monitored. These areas include aeronautics, health monitoring of complex structures, metallurgy, mechanics and many others. Nowadays, different types of sensors based on strain/ displacement measurement are being developed using fiber optic techniques.

1.2.3 Electric and Magnetic Field Sensors

In the electric power industry, there are high and low-tension structures present which requires high and accurate electric and magnetic field sensing. Due to the presence of metallic content in conventional sensors in the form of conductive electrodes, antennas and other metallic contents, there are chances of high perturbance in the measured parameters.[9] ,

1.2.4 Pressures Sensors

In various industrial applications, there is requirement of pressure measurements in the presence of extremely harsh environmental conditions like material processing systems, turbine engines, gas and oil exploitations, compressors and power plants and material processing systems. Fiber optic pressure sensors work successfully in harsh environments because of their high operation temperature, high sensitivity, immunity to electromagnetic interference wide bandwidth, and lightweight.[10], [11], [12]

1.2.5 Temperature Sensors

Fiber optic-based sensors are very useful in determining temperature in particular turbine areas specially in the generation of power operations in basic glass and metal productions, sintering operations, automated welding equipment's, furnaces of all sorts, and ovens. Other applications include high temperature processing in cemant and chemical industries. The use of temperature sensors in semiconductor industry uses temperature sensing technique of FO in crystal processes, fusion, and sputtering. Industries such as aerospace, defense and civil use purpose.[13]

1.2.6 Refractive Index Sensors

One of the basic fundamental material property is refractive index. Consequently, the accurate measurement of refractive index is important in many applications. The monitoring of refractive index is essential for quality control in food and beverage industries. Optical fiber based refractive index sensors have flexibility in their design, network compatibility, immunity to EMI, aptitude for remote sensing, and small size.

1.3 Mathematical analysis of Photonic Crystal Fiber

1.3.1 Effective refractive index

It is a measurement of overall delay of a light beam propagating in an optical medium.

$$\beta = \eta_{eff}\frac{2\pi}{\lambda} \tag{1.4}$$

Where β is propagation constant, η_{eff} is effective refractive index and λ is wavelength.

1.3.2 Modal Birefringence

Refractive index is also dependent on the propagation direction and polarization state of the light so it is not same for the two fundamental nodes (x and y mode). The difference between their values is termed as birefringence. [32]

$$birefringence = \mid \eta_{eff}(xmode) - \eta_{eff}(ymode) \mid \tag{1.5}$$

1.3.3 Confinement loss

Due to presence of the finite number of holes, there is penetration of light into the cladding region which leads to loss termed as confinement loss defined by

$$\alpha_{loss} = \frac{40\pi}{\lambda ln10} Im(\eta_{eff}) \times 10^6 \left(\frac{dB}{m}\right) \tag{1.6}$$

Im (η_{eff}) represents the imaginary part of the effective mode index and λ represents the wavelength of light.

1.3.4 Relative Sensitivity

The interaction between sample and light is measured by calculating relative sensitivity coefficient defined by

$$r = \frac{n_r}{\eta_{eff}} \times f \tag{1.7}$$

n_r is the refractive index of liquid analyte that present in the core, η_{eff} is the effective

mode index and f is the percentage of the ratio of core power and the total power in the fiber.

1.4 Hexagonal Geometry

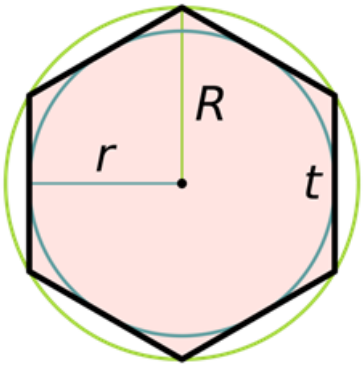

Figure 1.6: Figure showing Hexagonal geometry specification

In figure 1.6, the maximum value of diameter D, is twice the maximal radius or circumradius, R, and R equals the side length, t. The minimum value of diameter or the diameter of the inscribed circle d, is twice the minimal radius or inradius, r .

Chapter 2

COMSOL Multiphysics

COMSOL Multiphysics is a simulation software used for solving engineering problems by modelling, solving and analyzing them. It is based on solving Partial Differential Equations (PDE) by Finite Element Method(FEM).

Figure 2.1: Cosmol multiphysics

FEM is a numerical method of solving engineering and mathematical physics. It consists of algebraic equations. The whole unit is divided into small fragments called Finite element and each individual element's PDE are solved along with applying boundary values. Then, all the minimized PDEs are grouped into larger system of equations to address the whole issue. It is done in order to get a optimum solution with minimized error.

Basic steps:

1. Choosing a model: New Model (shown in figure 2.2)

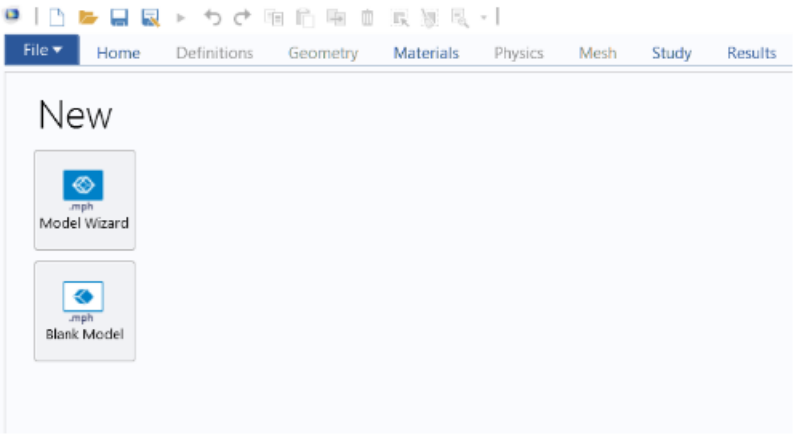

Figure 2.2: Model selection in cosmol

2. Choosing the dimension of geometry: 2D symmetrical (shown in figure 2.3)

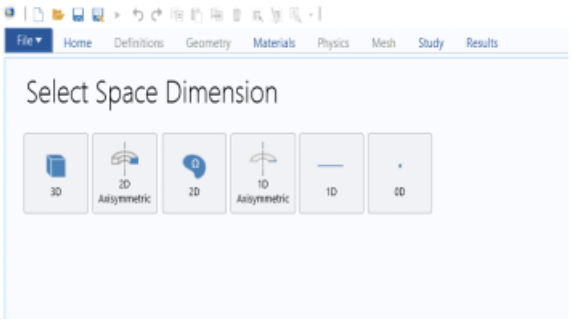

Figure 2.3: Choosing dimension of geometry in cosmol

3. Adding the Physics: Wave optics – frequency domain(shown in figure 2.4)

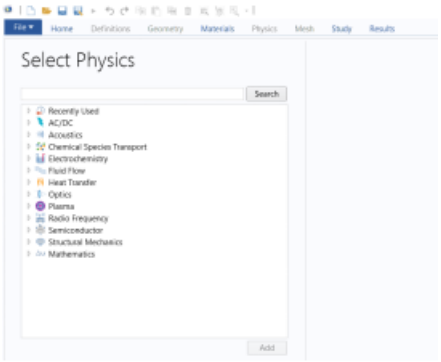

Figure 2.4: Physics selection in cosmol

4. Adding the predefined values of variables used for designing the geometry: parameters

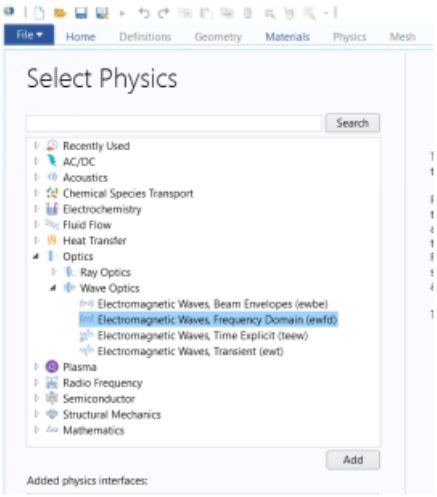

Figure 2.5: Choosing physics domain in cosmol

5. Creating the geometry

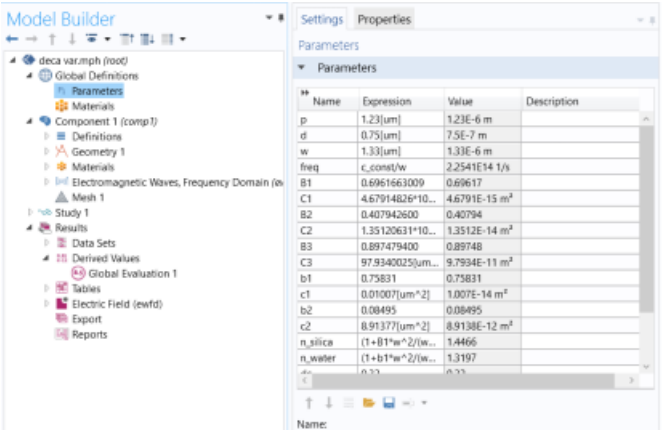

Figure 2.6: Adding parameters

6. Adding the materials: silica, air and analyte to be tested

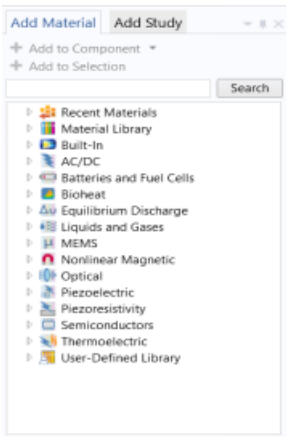

Figure 2.7: Addition of Materials

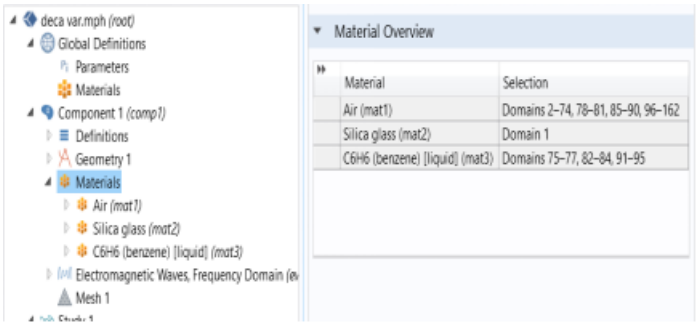

Figure 2.8: Material Selection

7. Adding the study: mode analysis

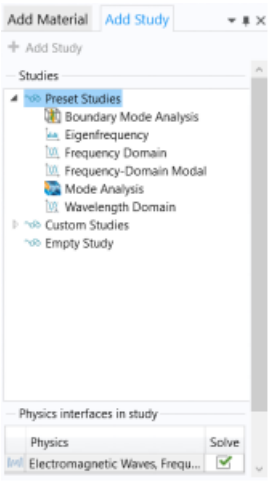

Figure 2.9: Choosing study

8. Creating a mesh : physics controlled mesh – finite element size

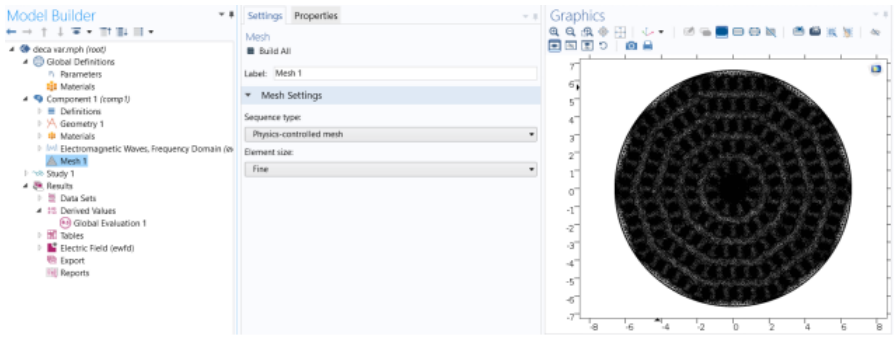

Figure 2.10: Meshing of the geometry

9. Simulating: study – no of modes to be searched=2, modes to be searched around = n_ethanol (value added in parameters), mode analysis frequency= freq (value mentioned in parameters) – compute

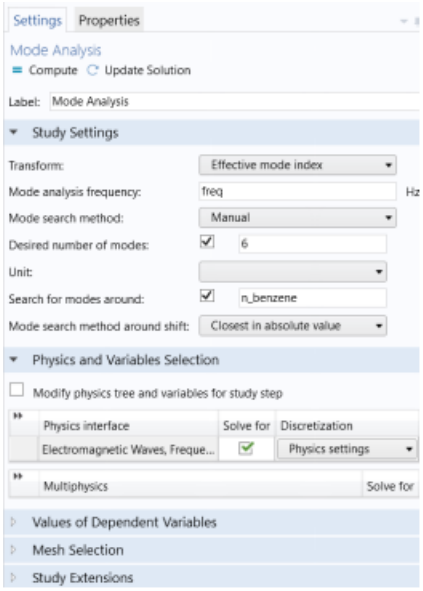

Figure 2.11: Computing the geometry

10. Studying the results: global evaluation – generating the values of effective refractive index and fill fraction

Figure 2.12: Global evaluation of variables

11. Importing the values to excel for further analysis.

Chapter 3

Design of Hexagonal PCF with circular holes and eliptical holes

In this chapter, the hexagonal geometry that have been studied are listed. A hexagonal microstructured PCF has been designed, where air holes which constitute the cladding, are arranged in a hexagonal pattern with pitch (hole to hole space, represented by $\wedge$) is 1.63 μm and Diameter of small holes is 0.57 μm and Diameter of large holes is 1.5 μm. For hexagonal geometry, vertices of adjoining air holes contain 60^0 angles. There are total 3 rings in the geometry. Analysis of this structure is performed at wavelength 1.55 μm.The cross-sectional view of designed hexagonal fiber is shown in fig 3.1. [7], [14], [15], [16], [4]

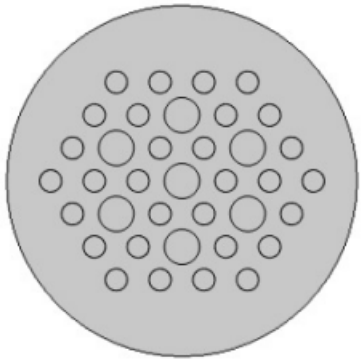

Figure 3.1: Inner core circular geometry hexagonal with x-axis as major axis

Again, the large holes are filled with the liquid analyte Benzene and these geometries are tested with the help of COMSOL Multiphysics Software. The values of Dispersion,

effective refractive index and confinement loss is taken and compared with above geometries. The graphs showing the comparison for different geometries have been plotted and the results obtained for 1.33μm wavelength have been stated in the tabular form for easy analysis.[6], [5]

Benzene modal analysis:

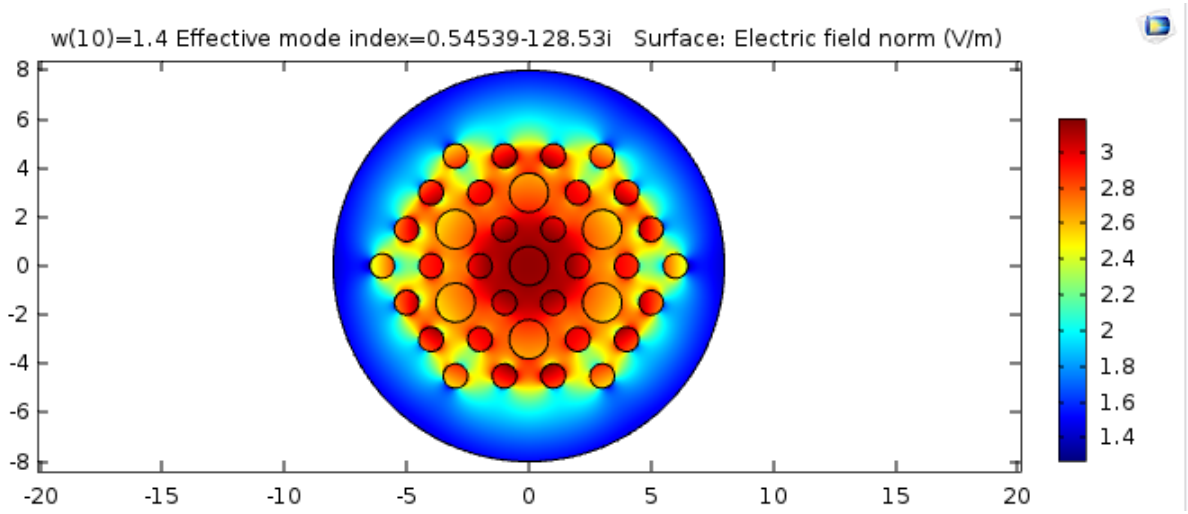

Figure 3.2: Electrical mode field analysis for Benzene

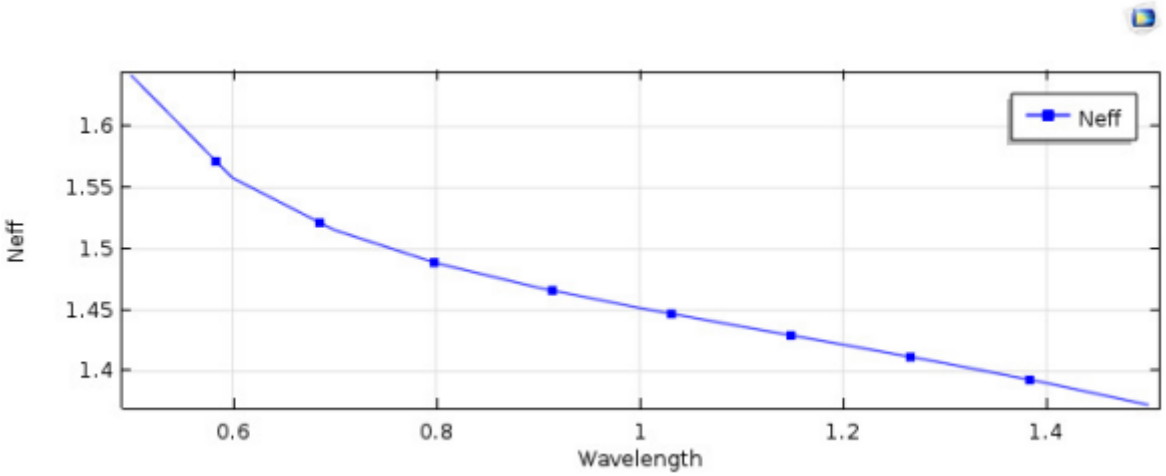

Figure 3.3: η_{eff} vs wavelength for benzene filled core in various geometries hexagonal with x-axis as major axis

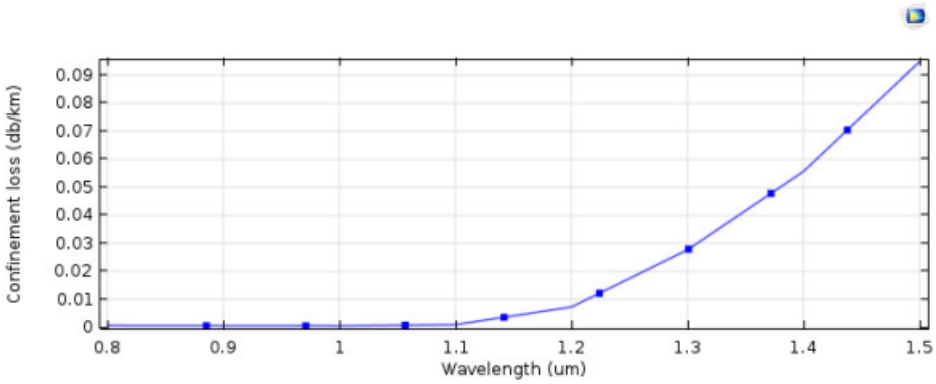

Figure 3.4: Confinement loss vs wavelength for benzene filled core in various geometries a) Hexagonal with x-axis as major axis

From the above graphs for the geometries filled with benzene, it can be seen that the Confinement loss is firstly increasing with wavelength slowly and then increasing very sharply and η_{eff} is decreasing sharply. The Confinement loss and η_{eff} values are in the order hexagonal with x-axis as major axis. The Confinement loss values is 0.41783829 dB/km for hexagonal with x-axis as major axis at 1.30μm wavelength. The η_{eff} values are 1.469 for hexagonal with x-axis as major axis, at 1.33μm wavelength.[7], [17]

The dispersion value can be seen from the graph and these values are ploted against wavelength and from the graph it is clear that we got the zero dispersion value at the value of wavelength 1.6 μm so this wavelength is also called the Zero Dispersion Wavelength.[18], [19]

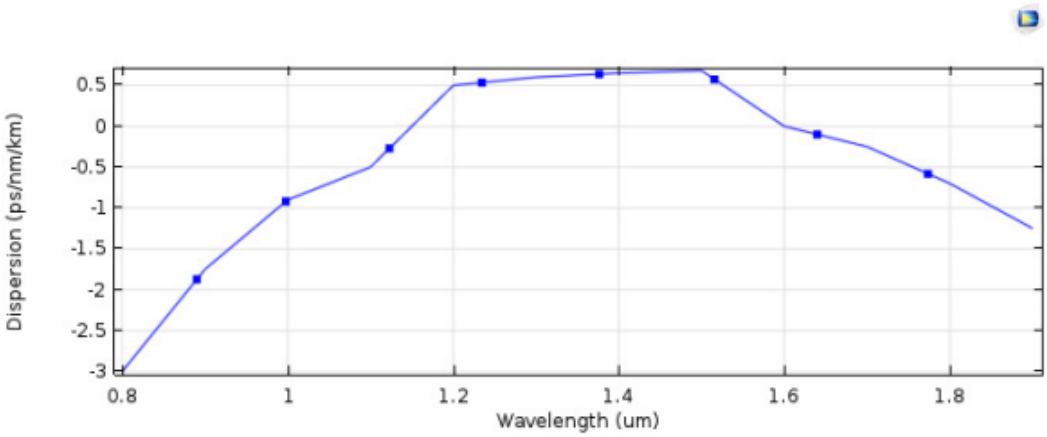

Figure 3.5: Dispersion vs wavelength for benzene filled core in Hexagonal geometry with x-axis as major axis

3.1 Hexagonal Structure with One inner ring of elliptical holes filled with Benzene

In this structure , the hexagonal geometry that have been studied are listed. A hexagonal microstructured PCF has been designed, where air holes which constitute the cladding, are arranged in a hexagonal pattern with pitch (hole to hole space, represented by $\wedge$) is 1.63 μm and in this geometry the diameter of small holes is 0.57 μm and Diameter of large holes is 1.5 μm and here replaced the inner ring of Circular air holes with Elliptical air holes and filled the large holes with Benzene.For hexagonal geometry, vertices of adjoining air holes contain 60^0 angles. There are total 3 rings in the geometry.

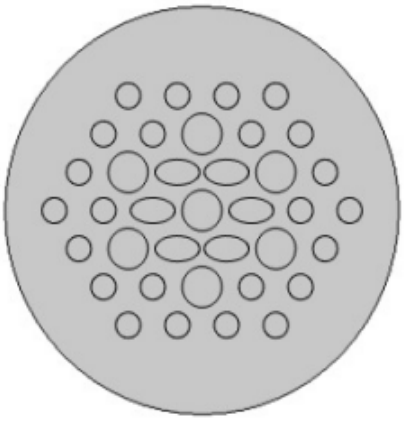

Figure 3.6: inner core circular geometry hexagonal with x axis as major axis

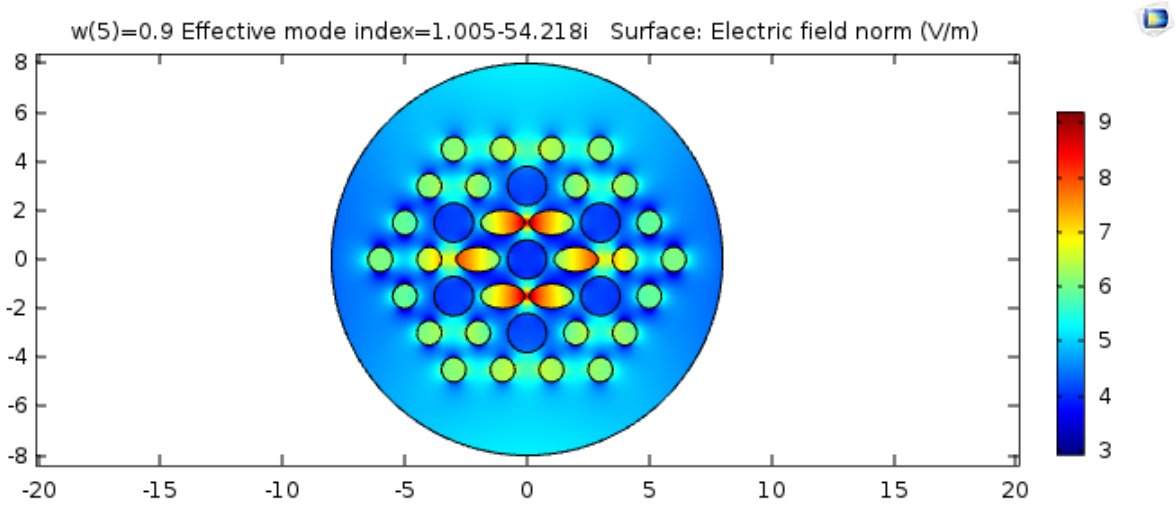

Figure 3.7: Electrical mode field analysis for one ring of elliptical holes(Benzene)

3.1. Hexagonal Structure with One inner ring of eliptical holes filled with Benzene

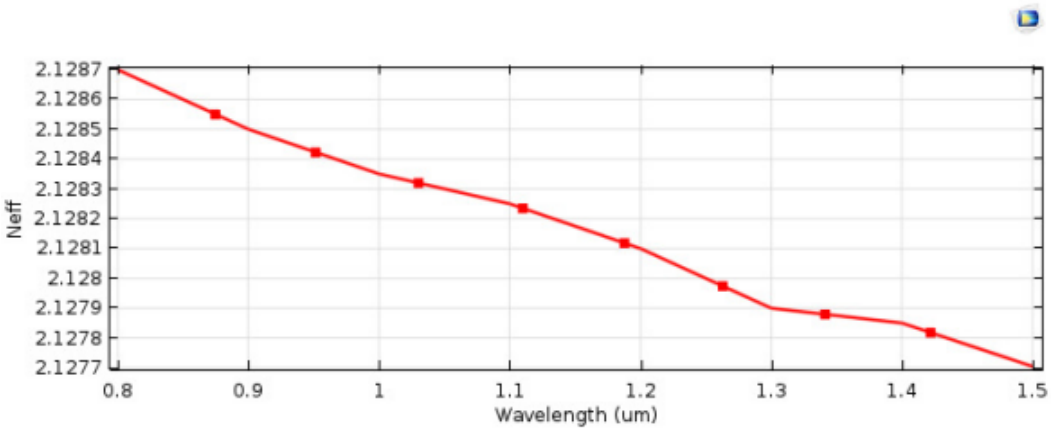

Figure 3.8: η_{eff} vs wavelength for ethanol filled core in various geometries hexagonal with x-axis as major axis

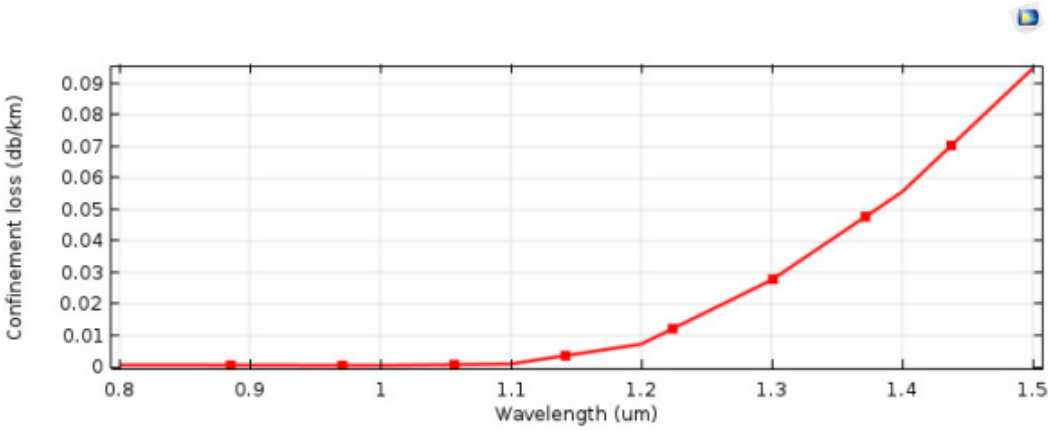

Figure 3.9: Confinement loss vs wavelength for ethanol filled core in various geometries hexagonal with x-axis as major axis

From the above graphs for the geometries filled with ethanol, it can be seen that the sensitivity is slightly decreasing with wavelength and η_{eff} is decreasing sharply. The η_{eff} values are in the increasing order: hexagonal with x-axis as major axis, but the confinement loss first increases very slowly with wavelength and after a particular wavelength the value of Confinement loss increases very sharply.

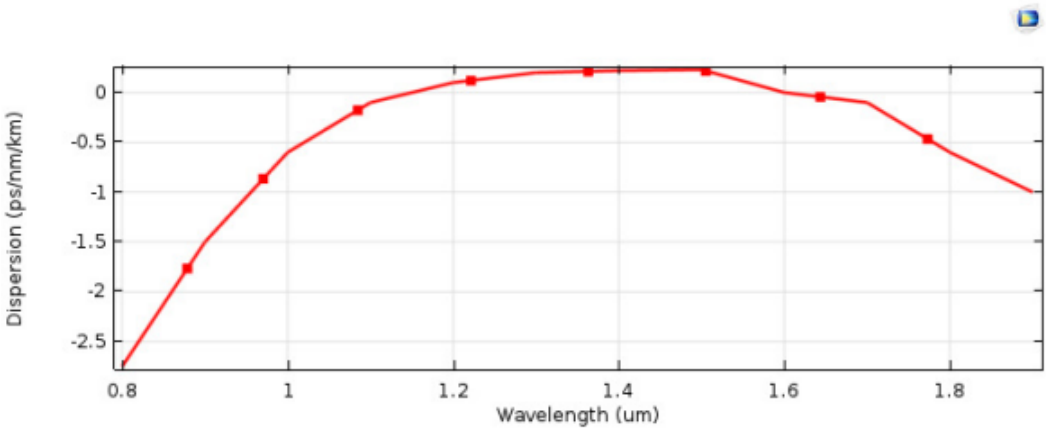

Figure 3.10: Dispersion vs wavelength for ethanol filled core in various geometries Hexagonal with x-axis as major axis

The dispersion value can be seen from the graph and these values are ploted against wavelength and from the graph it is clear that we got the zero dispersion value at the value of wavelength 1.6 μm so this wavelength is also called the Zero Dispersion Wavelength.

3.2 Hexagonal Structure with all inner rings of eliptical holes filled with Benzene

In this structure , the hexagonal geometry that have been studied are listed. A hexagonal microstructured PCF has been designed, where air holes which constitute the cladding, are arranged in a hexagonal pattern .In this Structure all the rings of Circular air holes are replaced with the rings of Elliptical air holes and the value of Semi major axis is 0.9 μm and Semi minor axis is 0.5 μm and the larger holes are filled with Benzene.

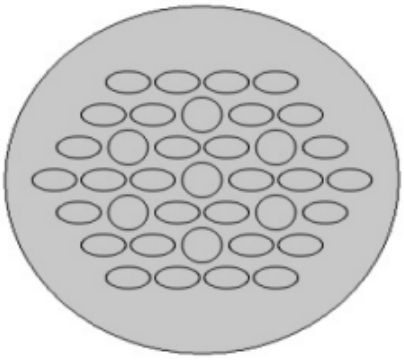

Figure 3.11: inner core eliptical hexagonal geometry with x axis as major axis.

3.2. Hexagonal Structure with all inner rings of eliptical holes filled with Benzene

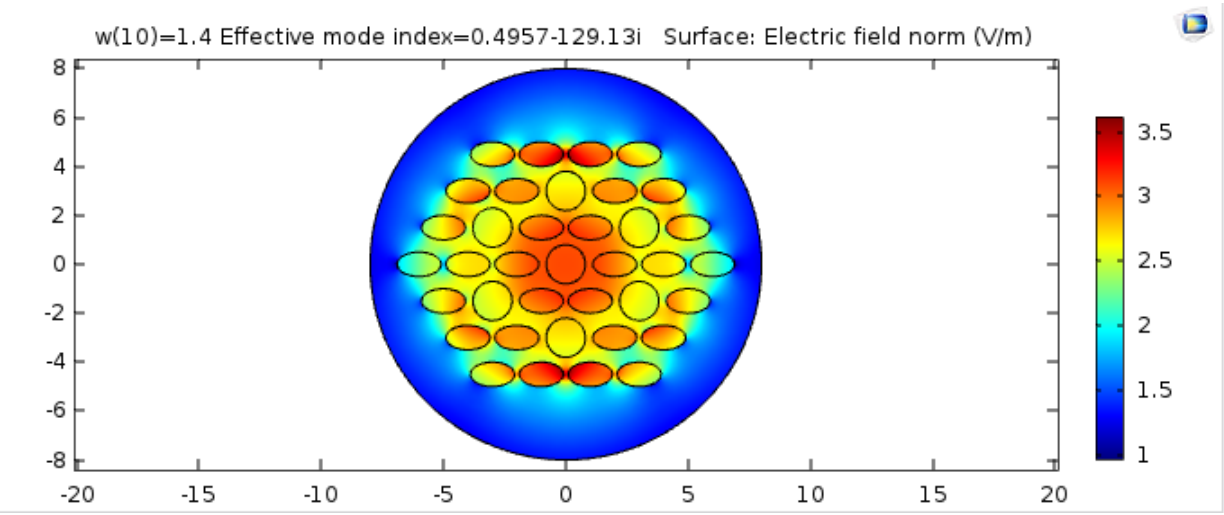

Figure 3.12: Electrical mode field analysis for all rings of elliptical holes(benzene).

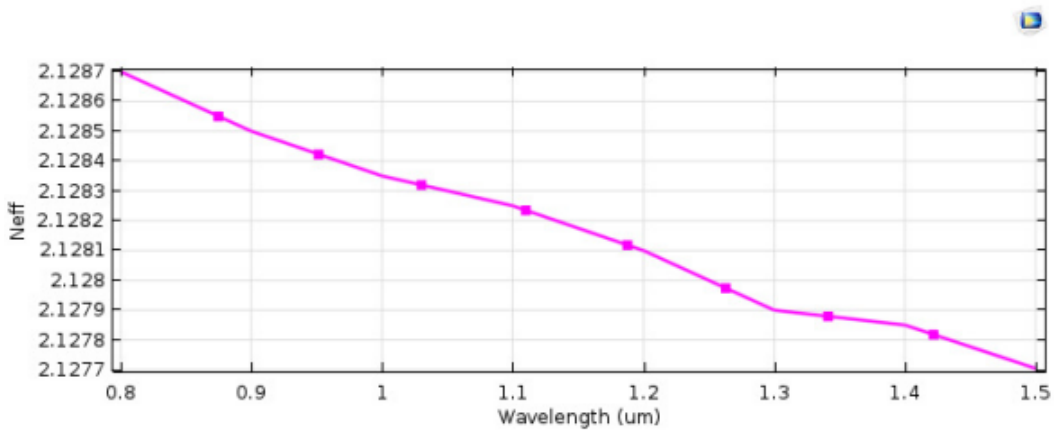

Figure 3.13: η_{eff} vs wavelength for water filled core in various geometries hexagonal with x-axis as major axis.

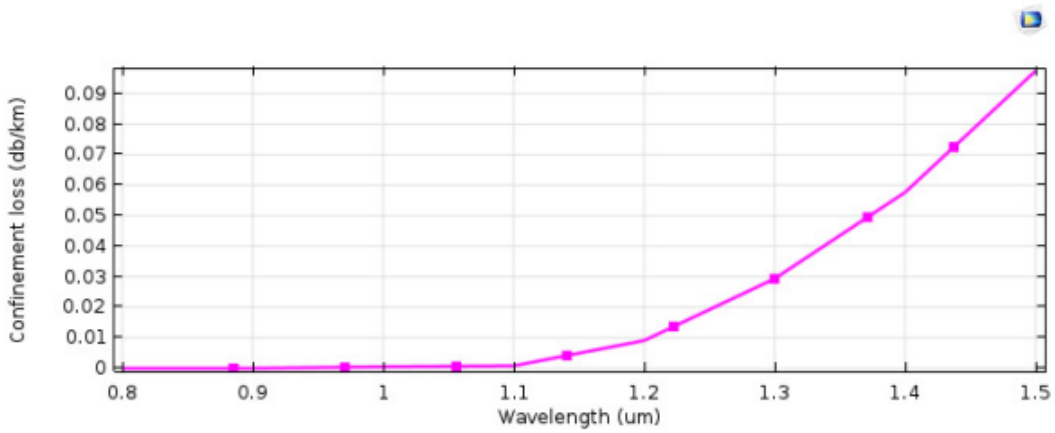

Figure 3.14: Confinement loss vs wavelength for water filled core in various geometries hexagonal with x-axis as major axis.

From the above graphs for the geometries filled with Benzene it can be seen that the Confinement loss is slightly increasing with wavelength and after a particular wavelength Confinement loss increases with wavelength very sharply and η_{eff} is decreasing sharply. The η_{eff} values are in the increasing order: hexagonal with x-axis as major axis. The η_{eff} values are 1.313 for hexagonal with x-axis as major axis, at 1.33μm wavelength.

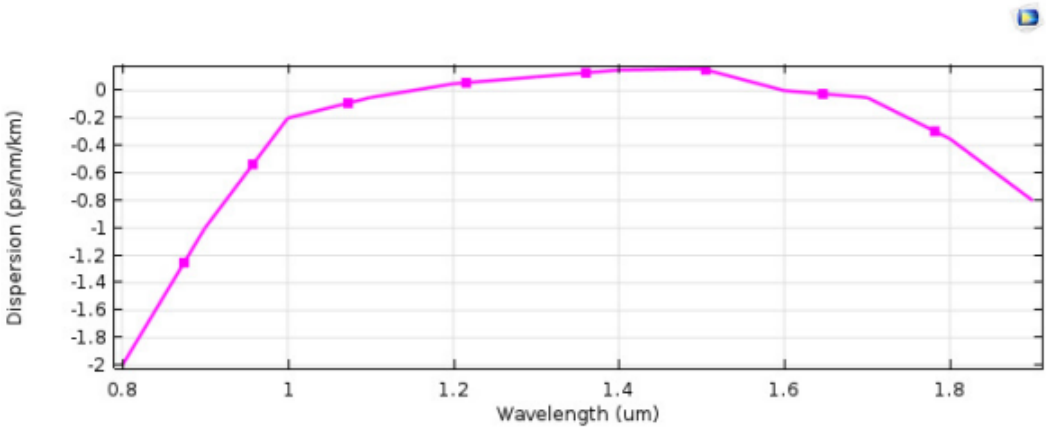

Figure 3.15: Dispersion vs wavelength for Benzene filled core in various geometries hexagonal with x-axis as major axis.

The dispersion value can be seen from the graph and these values are ploted against wavelength and from the graph it is clear that we got the zero dispersion value at the value of wavelength 1.65 μm so this wavelength is also called the Zero Dispersion Wavelength. The dispersion value obtained for the structure where all the rings of Elliptical Air holes filled with benzene is less than other two structure.

Chapter 4

Design of Hexagonal PCF with circular & eliptical holes (Ethanol)

In this chapter, the geometries that have been studied are listed. A Hexagonal microstructured PCF has been designed, where air holes which constitute the cladding, are arranged in a Hexagonal pattern with pitch (hole to hole space, represented by $\wedge$) is 1.65 μm and the Diameter of the smaller holes is taken as 0.57 μm and the diameter of the larger holes is taken as 1.5 μm. Here the analysis of this structure is performed at Wavelength 1.55 μm. For Hexagonal geometry, vertices of adjoining air holes contain 60^0 angles. There are total 3 rings in the geometry. The cross-sectional view of designed octagonal fiber is shown

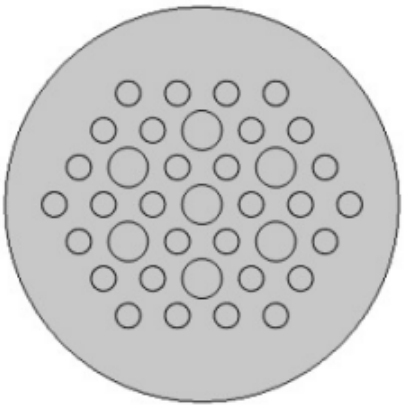

Figure 4.1: 1 Design of Hexagonal Structure with circular holes filled with Water.

The PCF is simulated using software COMSOL Multiphysics and the values of Dis-

persion,effective refractive index and confinement loss is observed over a wide range of wavelength. The values obtained for different analytes are compared with one another and represented in graphs.[20], [17], [21]

At first, simple geometry as shown in figure is simulated with inner core filled with benzene and the snapshots of modal confinement are shown below at 1.33 μm wavelength.

4.1 Ethanol Modal Analysis

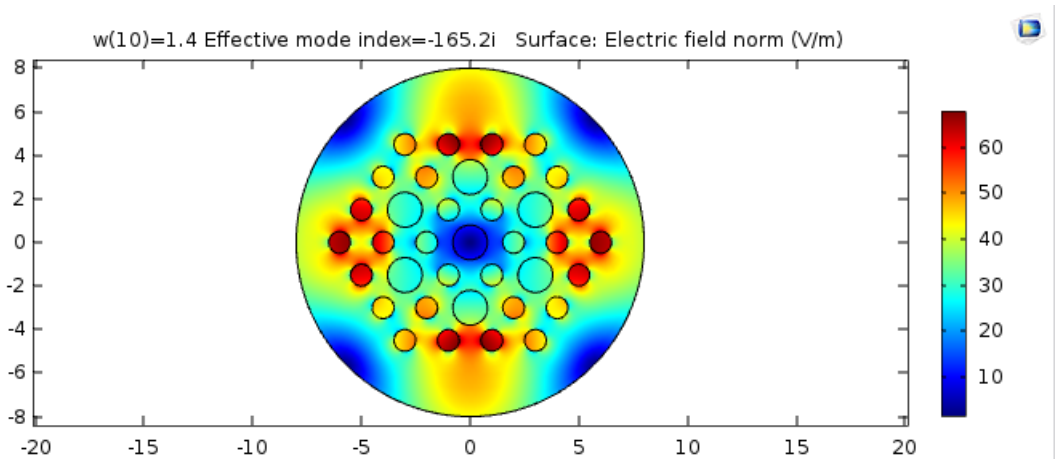

Figure 4.2: electrical mode field analysis for cirular holes(Ethanol)

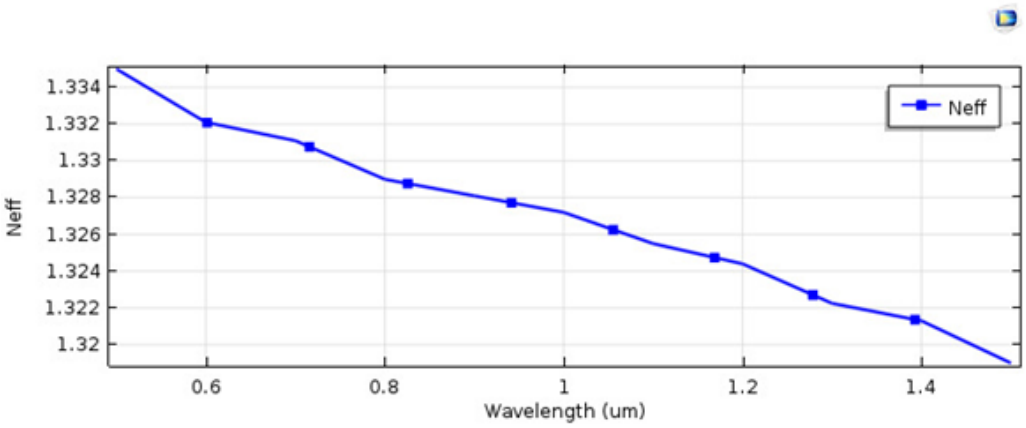

Figure 4.3: Effective refractive index versus wavelength(um) octagonal structure at (a) w=1.3μm (b) w=1.5μm

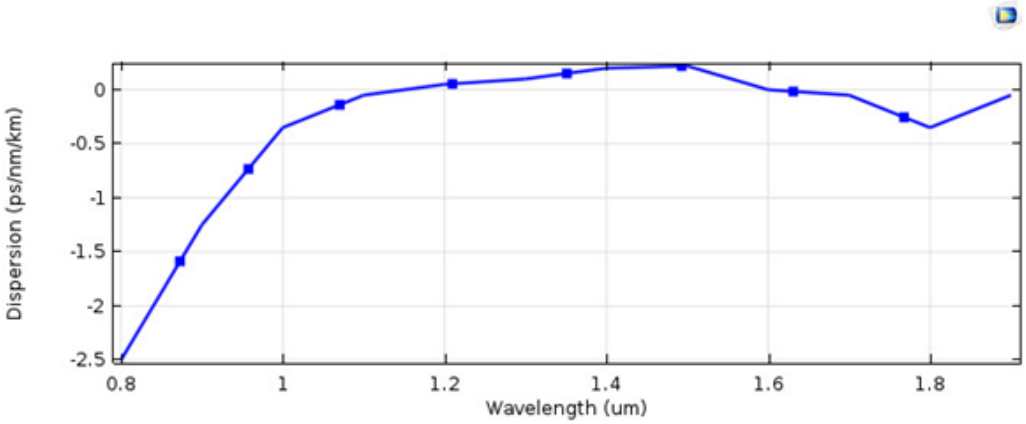

Figure 4.4: Dispersion versus wavelength(um) Hexagonal structure at w=1.3μm

From the above graphs for the geometries filled with benzene, it can be seen that the Dispersion first increasing with wavelength and after some value of wavelength the dispersion becomes zero and the value of this wavelength is known as zero dispersion wavelength and for this structure the wavelength value is approx is 1.66μm and η_{eff} is decreasing sharply. The η_{eff} values are in the increasing order. The Dispersion values are 0 ps/nm/km for Hexagonal with x-axis as major axis, at 1.63μm wavelength. The η_{eff} values are 1.4761 for Hexagonal with x-axis as major axis,at 1.33μm wavelength.[2], [2], [22]

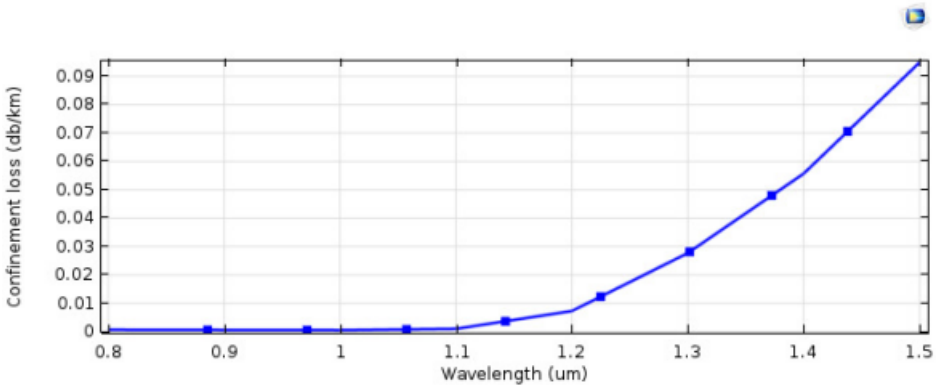

Figure 4.5: Confinement loss versus wavelength(um) of octagonal structure at w=1.3μm

The confinement loss as can be seen from the graph is negligible which states that the geometries used are able to confine most of the light into the core thus making it highly sensitive and reliable. The values for confinement loss are $0.54e^{-10}$dB/m at 1.33μm wavelength.

4.2 Hexagonal Structure with inner ring eliptical holes filled with Ethanol

In this structure , the hexagonal geometry that have been studied are listed. A hexagonal microstructured PCF has been designed, where air holes which constitute the cladding, are arranged in a hexagonal pattern with pitch (hole to hole space, represented by $\wedge$) is 1.63 μm and in this geometry the diameter of small holes is 0.57 μm and Diameter of large holes is 1.5 μm and here replaced the inner ring of Circular air holes with Elliptical air holes and filled the large holes with Ethanol.For hexagonal geometry, vertices of adjoining air holes contain 60^0 angles. There are total 3 rings in the geometry.[8], [**?**]

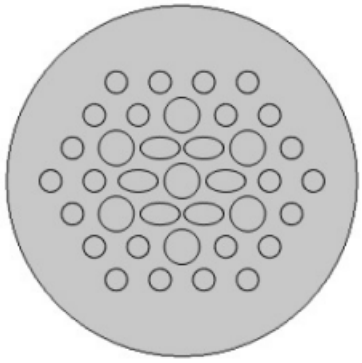

Figure 4.6: Design of Hexagonal structure with one ring of eliptical holes filled with Ethanol

4.2.1 mode analysis

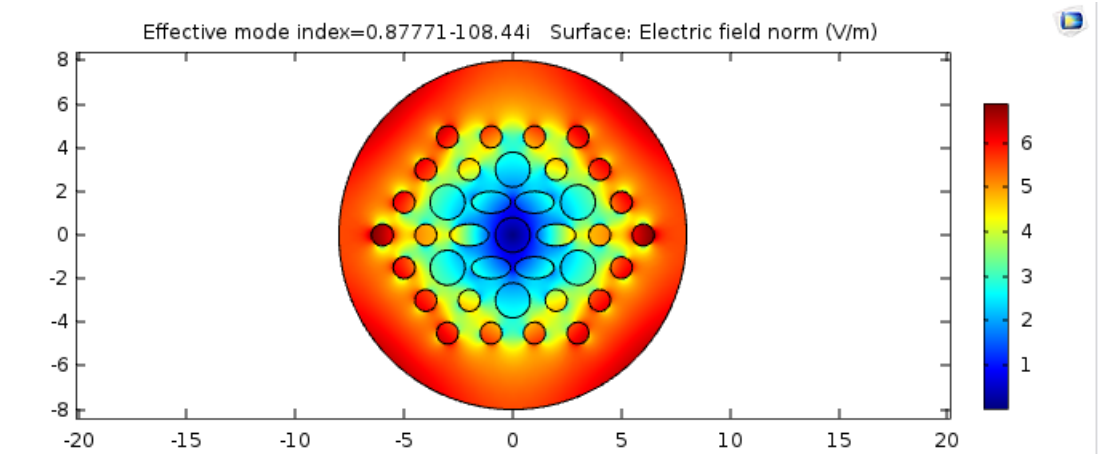

Figure 4.7: Electrical mode field analysis for one ring of elliptical holes(Ethanol)

4.2. Hexagonal Structure with inner ring eliptical holes filled with Ethanol

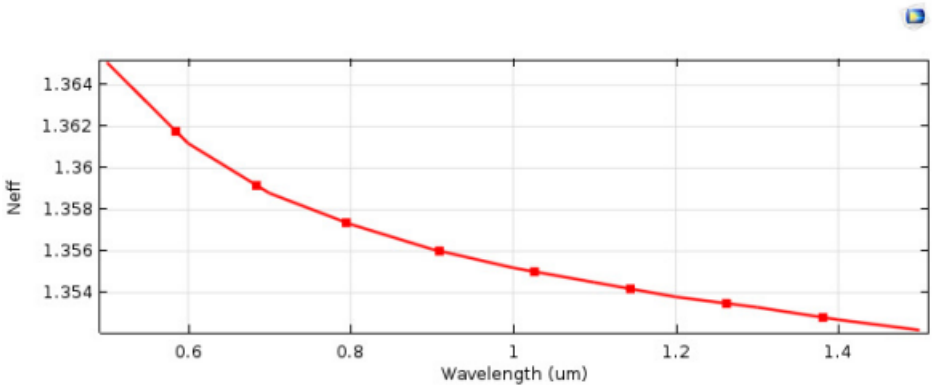

Figure 4.8: Effective refractive index versus wavelength(um) octagonal structure at w=1.3μm

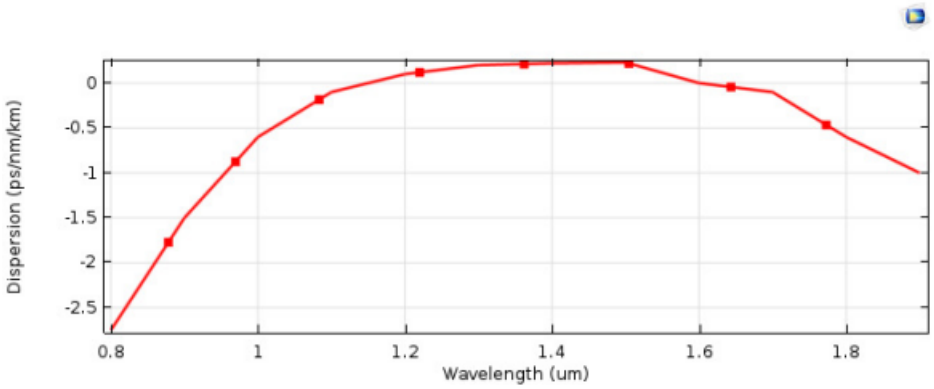

Figure 4.9: Dispersion versus wavelength(um) Hexagonal structure at w=1.3μm

From the above graphs for the geometries filled with Water, it can be seen that the Dispersion value first slowly increasing with wavelength and after a particular wavelength dispersion becomes zero this wavelength is known as zero dispersion wavelength and η_{eff} is decreasing sharply. η_{eff} are inversely proportional to each other as explained in equation 4. The η_{eff} values are 1.47 for hexagonal, at 1.33μm wavelength

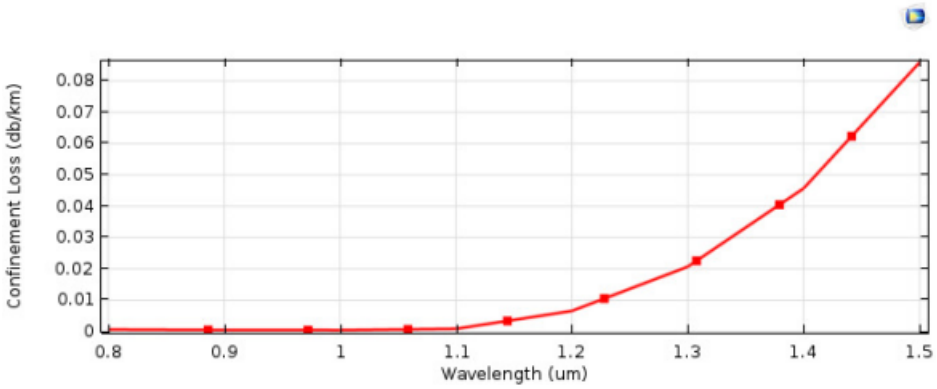

Figure 4.10: Confinement loss versus wavelength(um) of octagonal structure at w=1.3μm

The confinement loss as can be seen from the graph is negligible which states that the geometries used are able to confine most of the light into the core thus making it highly sensitive and reliable. The values for confinement loss are $1.48e^{-14}$dB/m for decagonal at 1.33μm wavelength.

4.3 Hexagonal structure with all ring of eliptical holes filled with Ethanol

In this structure , the hexagonal geometry that have been studied are listed. A hexagonal microstructured PCF has been designed, where air holes which constitute the cladding, are arranged in a hexagonal pattern .In this Structure all the rings of Circular air holes are replaced with the rings of Elliptical air holes and the value of Semi major axis is 0.9 μm and Semi minor axis is 0.5 μm and the larger holes are filled with Ethanol.[1]

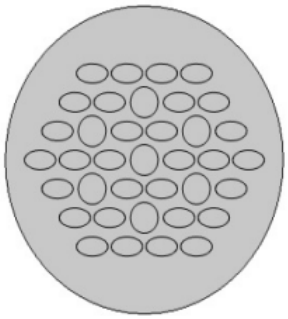

Figure 4.11: Design of Hexagonal structure with one ring of eliptical holes filled with Ethanol

4.3.1 Mode field Analysis

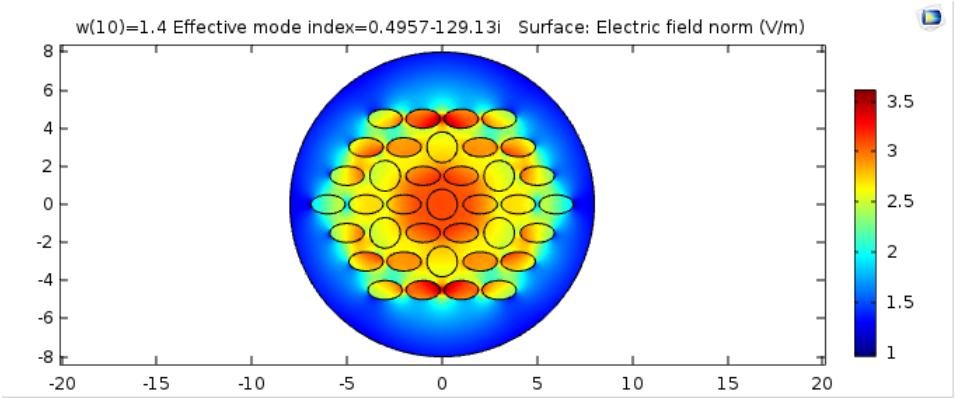

Figure 4.12: Electrical mode field analysis for all rings of elliptical holes(Ethanol)

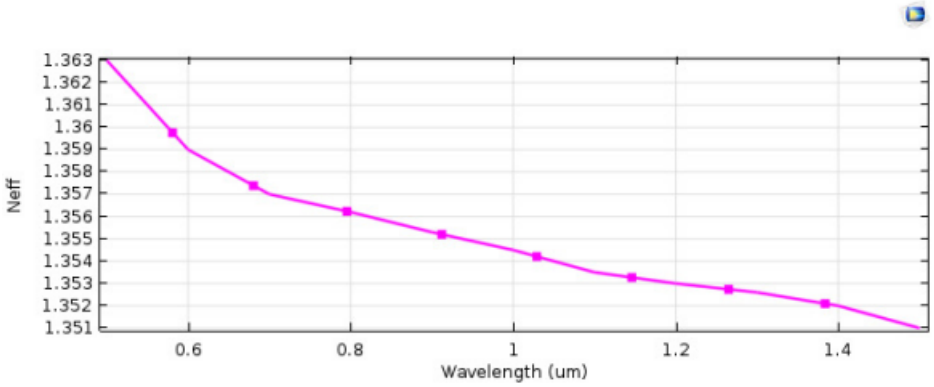

Figure 4.13: Effective refractive index versus wavelength(μm) hexagonal structure at w=1.3μm

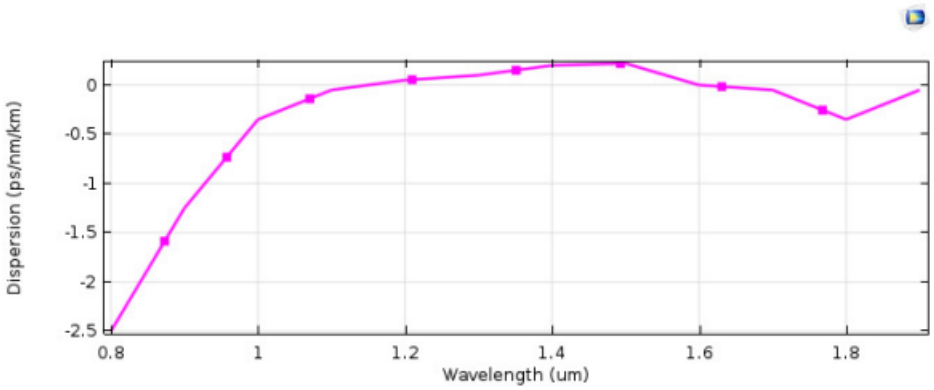

Figure 4.14: Dispersion versus wavelength(μm) Hexagonal structure at w=1.3μm

From the above graphs for the geometries filled with ethanol, it can be seen that the value of dispersion first increases with wavelength and after that at a particular wavelength the

dispersion value become zero this is known as zero dispersion wavelength and for this structure this value comes out 1.68 μm and η_{eff} is decreasing sharply. The η_{eff} values are in the increasing order hexagonal with x-axis as major axis. Theη_{eff} values are 1.3317 for octagonal with x-axis as major axis,at 1.33μm wavelength.

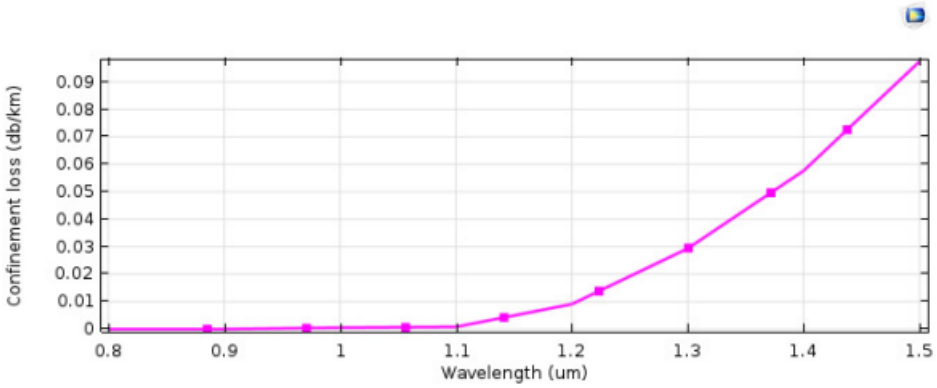

Figure 4.15: Confinement loss versus wavelength(um) of hexagonal structure at w=1.3μm

The confinement loss as can be seen from the graph is negligible which states that the geometries used are able to confine most of the light into the core thus making it highly sensitive and reliable. The values for confinement loss are 1.29e_{-09} dB/m octagonal with x-axis as major axis at 1.33μm wavelength.

Chapter 5

Design of Hexagonal PCF with circular, eliptical holes (Water)

In this chapter, the hexagonal geometry that have been studied are listed. A hexagonal microstructured PCF has been designed, where air holes which constitute the cladding, are arranged in a hexagonal pattern with pitch (hole to hole space, represented by $\wedge$) is 1.63 μm and Diameter of small holes is 0.57 μm and Diameter of large holes is 1.5 μm. [17],[2] For hexagonal geometry, vertices of adjoining air holes contain 60^0 angles. There are total 3 rings in the geometry. Analysis of this structure is performed at wavelength 1.55 μm.The cross-sectional view of designed hexagonal fiber is shown in fig 5.1. [23], [24]

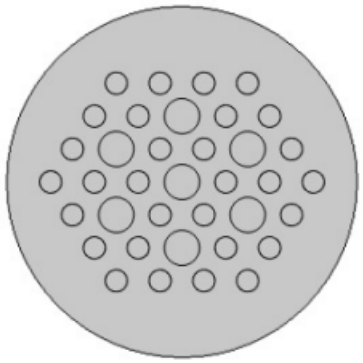

Figure 5.1: Design of Hexagonal Structure with circular holes filled with Water

The background material in the fiber is of silica which is filled by varying its refractive

index using Sellemeier's equation

$$n^2(\lambda) = 1 + \frac{B_1\lambda^2}{\lambda^2 - C_1} + \frac{B_2\lambda^2}{\lambda^2 - C_2} + \frac{B_3\lambda^2}{\lambda^2 - C_3}..... \tag{5.1}$$

where n(λ) is the refractive index of the material at the wavelength, $B_1, B_2, B_3, C_1, C_2, C_3$ are sellemeier's constants given in table:

Material	B_1	B_2	B_3	$C_1(\mu m^2)$	$C_2(\mu m^2)$	$C_3(\mu m^2)$
Silica	696166300	0.00467914826	0. 407942600	35120631	0.897479400	7.9340025

Table 5.1: Table Showing Sellemeier's coefficients of silica

The holes present in the cladding are filled with air and the inner core is filled with liquid analyte whose sensitivity is to be determined. Here, liquid analytes that are tested are ethanol, water and benzene.

5.0.1 Water Mode Field Analysis

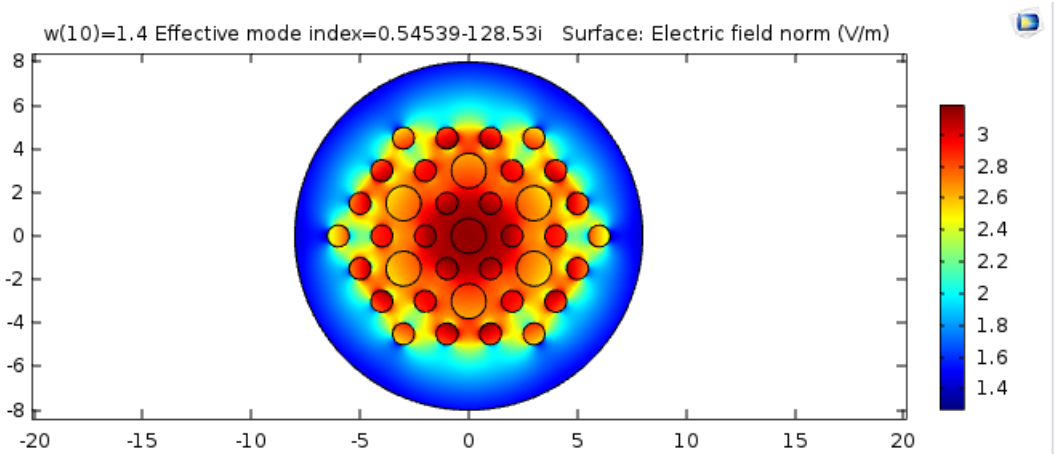

Figure 5.2: Electrical mode field analysis for circular holes(Water)

At first, simple geometry as shown in figure 5.3 is simulated with inner core filled with water and the snapshots of modal confinement are shown below at 1.33 μm wavelength

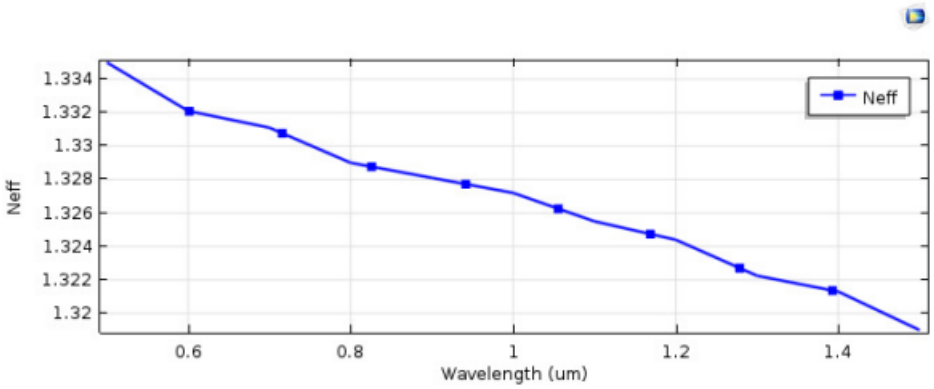

Figure 5.3: Refractive index variation with wavelength for water

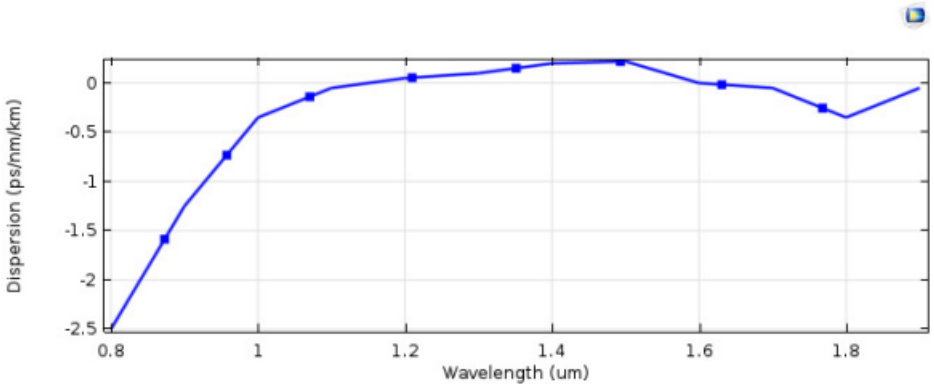

Figure 5.4: Dispersion versus wavelength(μm) hexagonal structure at w=1.3μm

η_{eff} is decreasing with wavelength in agreement with the equation which states that η_{eff} is inversely proportional to wavelength. It has higher value for denser medium as can be seen from the graph. The values of η_{eff} at 1.33μm wavelength are 1.375(μm) for water.

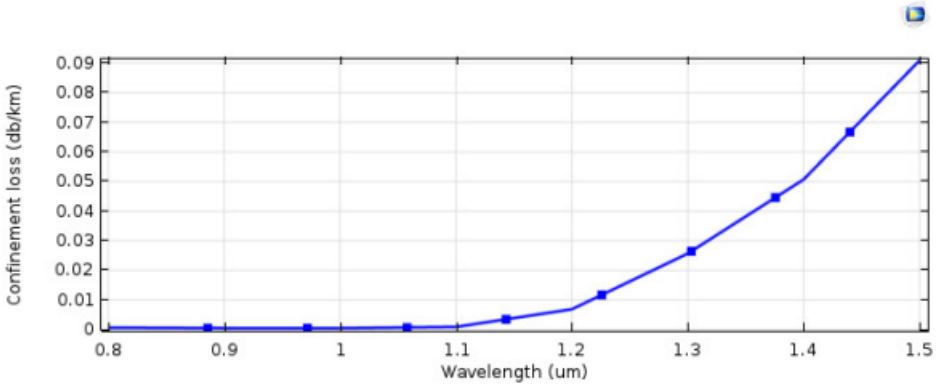

Figure 5.5: Confinement loss vs wavelength graph of core filled with water for geometry hexagonal

The confinement loss as can be seen from the graph is negligible which states that the geometries used are able to confine most of the light into the core thus making it highly sensitive and reliable. The values for confinement loss are $1.48e^{-14}$ dB/m for decagonal at $1.33\mu m$ wavelength.[25], [4], [26].

5.1 Hexagonal structure with one ring of eliptical holes filled with water

In this structure , the hexagonal geometry that have been studied are listed. A hexagonal microstructured PCF has been designed, where air holes which constitute the cladding, are arranged in a hexagonal pattern with pitch (hole to hole space, represented by $\wedge$) is 1.63 μm and in this geometry the diameter of small holes is 0.57 μm and Diameter of large holes is 1.5 μm and here replaced the inner ring of Circular air holes with Elliptical air holes and filled the large holes with Water.For hexagonal geometry, vertices of adjoining air holes contain 60^0 angles. There are total 3 rings in the geometry.

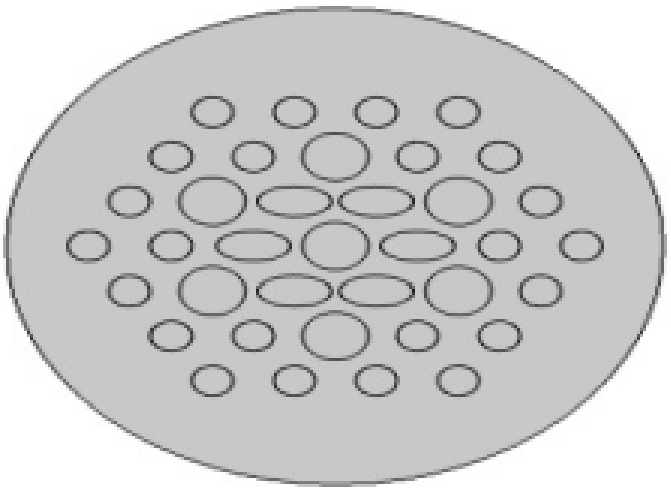

Figure 5.6: Design of Hexagonal Structure with one ring of eliptical holes filled with water

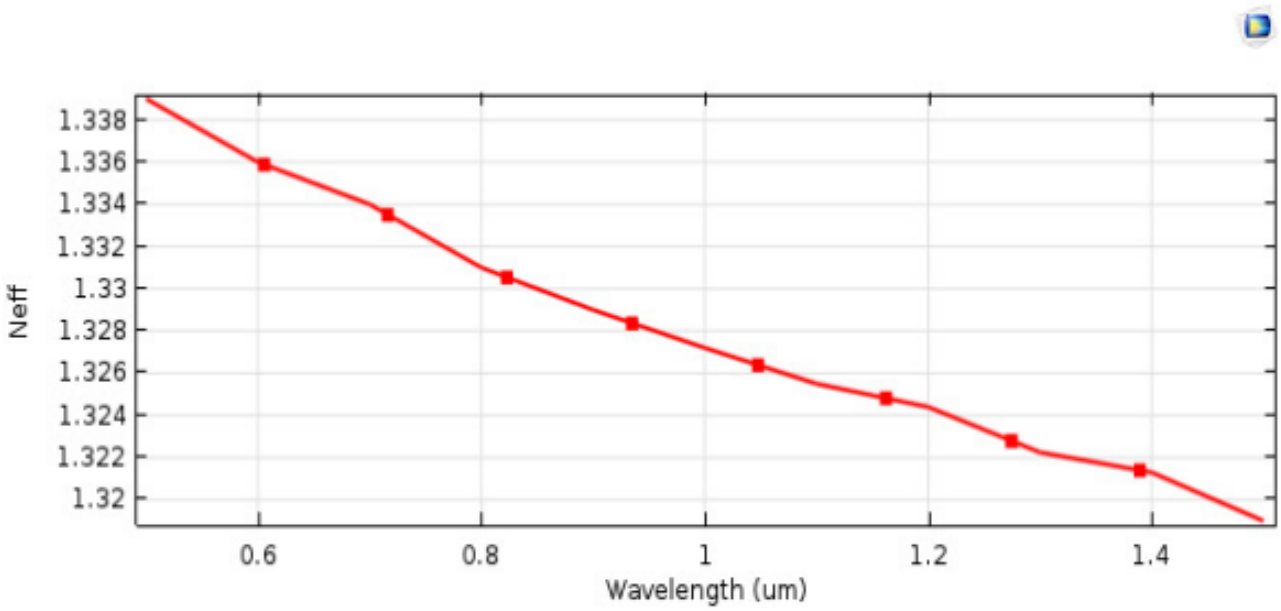

Figure 5.7: Effective refractive index versus wavelength(μm) Hexagonal structure at w=1.3μm

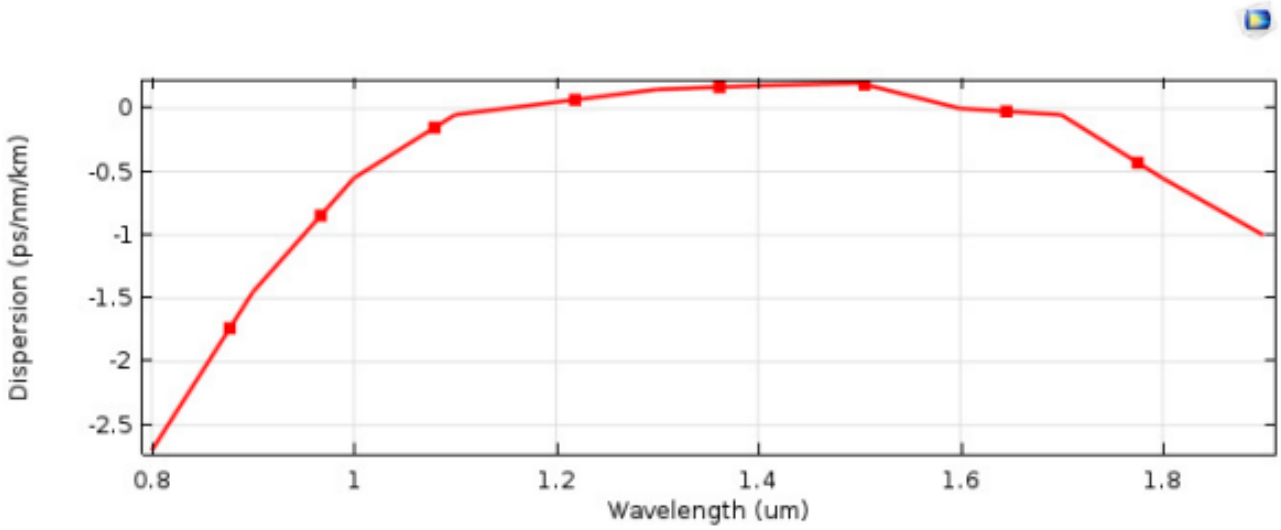

Figure 5.8: Dispersion versus wavelength(μm) hexagonal structure at w=1.3μm

From the above graphs for the geometries filled with Water, it can be seen that the Dispersion value first slowly increasing with wavelength and after a particular wavelength dispersion becomes zero this wavelength is known as zero dispersion wavelength and η_{eff} is decreasing sharply. η_{eff} are inversely proportional to each other as explained in equation 4. The η_{eff} values are 1.47 for hexagonal, at 1.33μm wavelength.

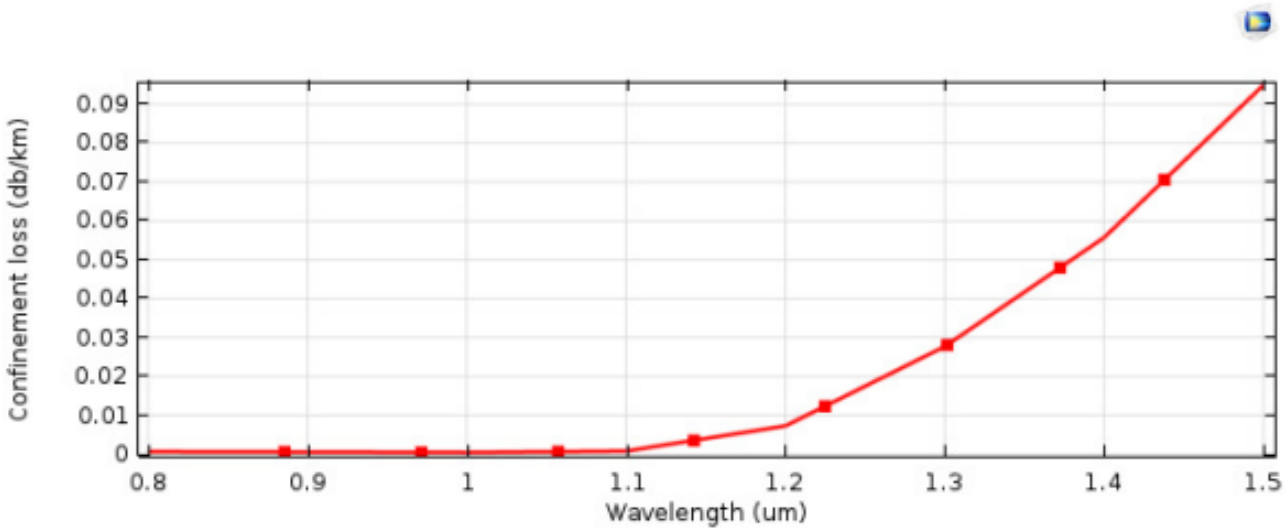

Figure 5.9: Confinement loss vs wavelength graph of core filled with benzene for geometry decagonal

The confinement loss as can be seen from the graph is negligible which states that the geometries used are able to confine most of the light into the core thus making it highly sensitive and reliable. The values for confinement loss are 1.48E-14 dB/m for decagonal at 1.33μm wavelength.[27], [28], [29]

5.2 Hexagonal Structure with all rings of eliptical holes filled with Water

In this structure , the hexagonal geometry that have been studied are listed. A hexagonal microstructured PCF has been designed, where air holes which constitute the cladding, are arranged in a hexagonal pattern .In this Structure all the rings of Circular air holes are replaced with the rings of Elliptical air holes and the value of Semi major axis is 0.9 μm and Semi minor axis is 0.5 μm and the larger holes are filled with Water.

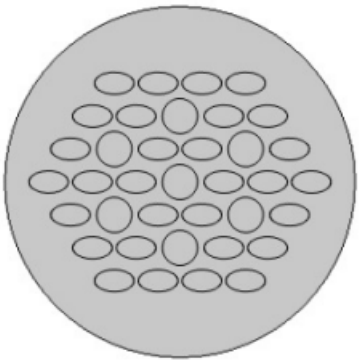

Figure 5.10: Design of Hexagonal structure with all rings of eliptical holes filled with Water

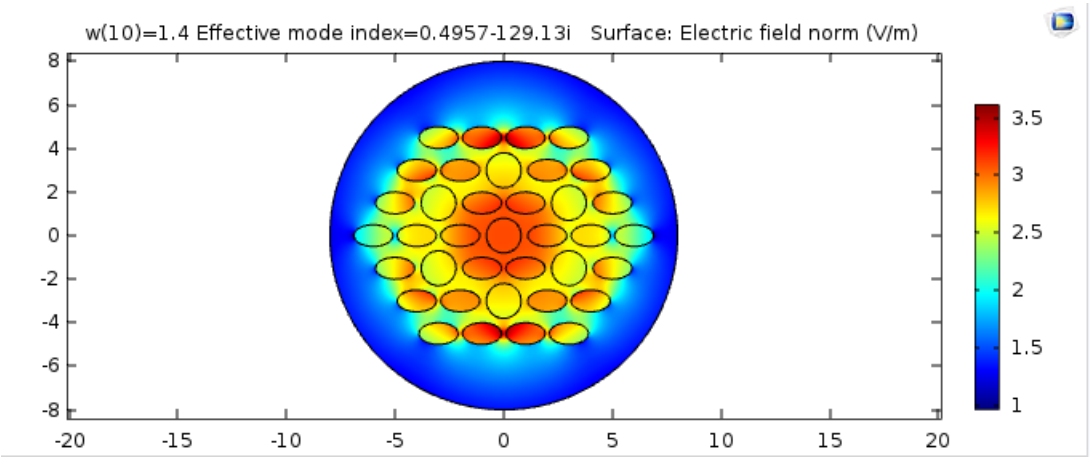

Figure 5.11: Electrical mode field analysis for all rings of elliptical hole(water)

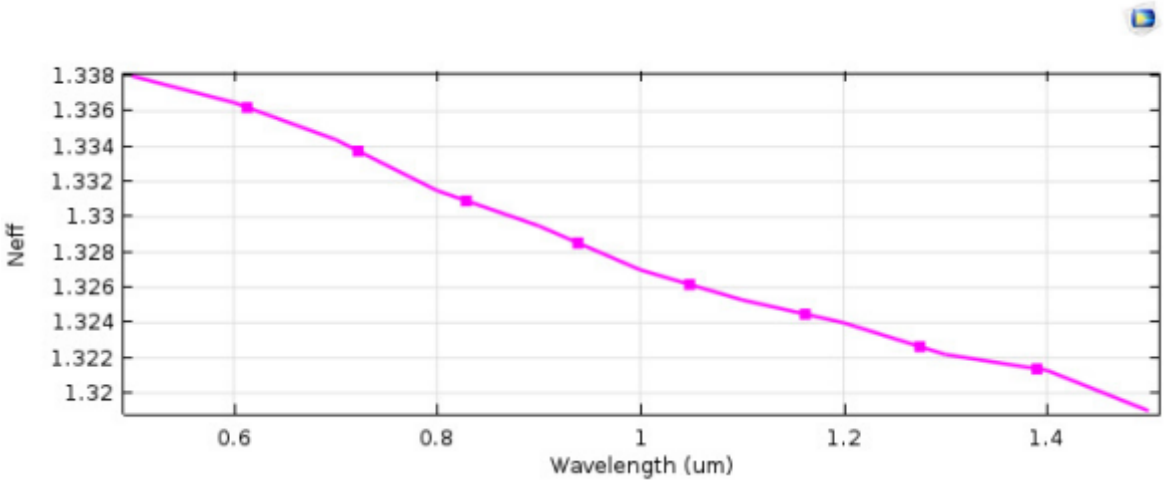

Figure 5.12: Effective refractive index versus wavelength(μm) Hexagonal structure at w=1.3μm

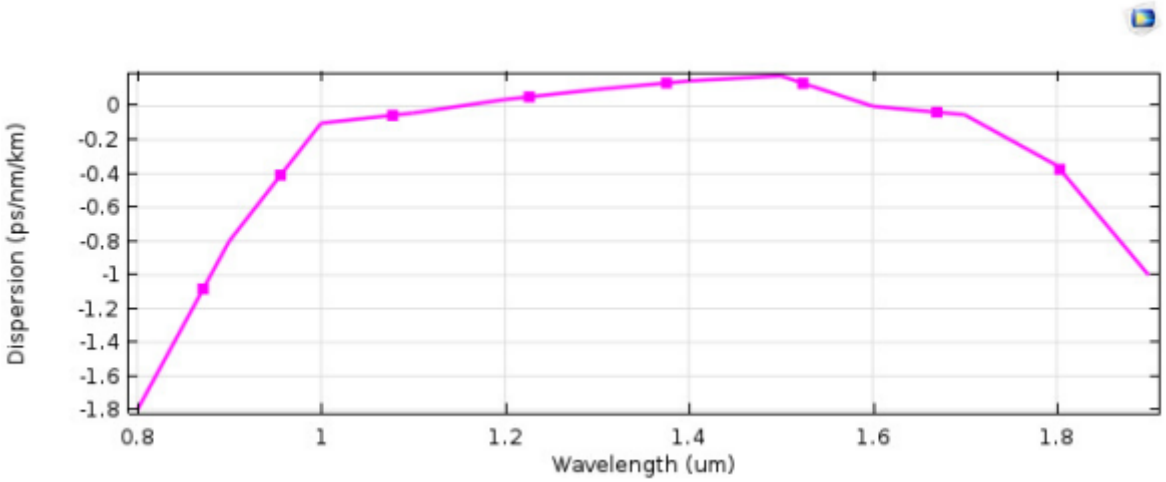

Figure 5.13: Dispersion Vs Wavelength plot

From the above graphs for the geometries filled with Water, it can be seen that the Dispersion value first slowly increasing with wavelength and after a particular wavelength dispersion becomes zero this wavelength is known as zero dispersion wavelength and η_{eff} is decreasing sharply. η_{eff} are inversely proportional to each other as explained in equation 4. The η_{eff} values are 1.47 for hexagonal, at 1.33μm wavelength.[13], [8].

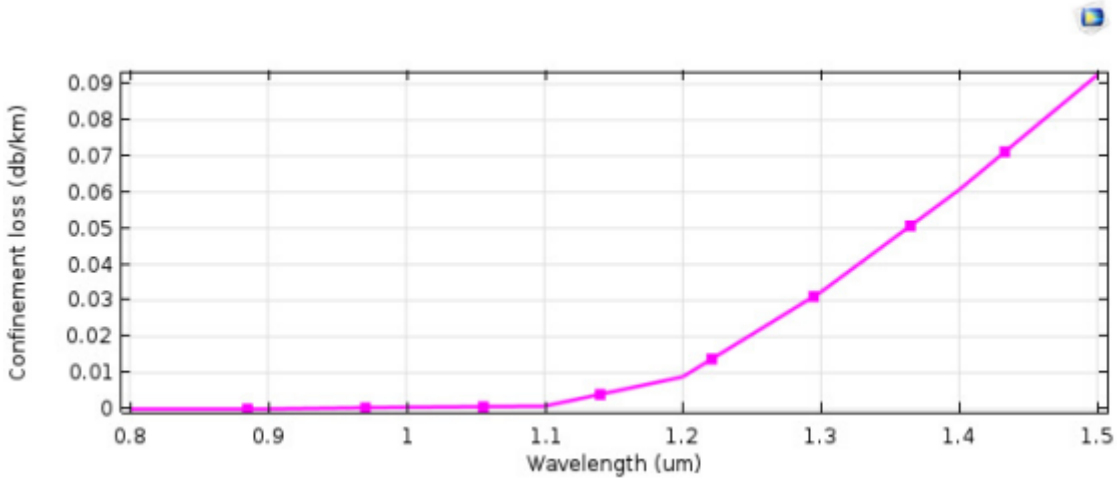

Figure 5.14: Confinement loss vs wavelength graph of core filled with water for geometry hexagonal

The confinement loss as can be seen from the graph is negligible which states that the geometries used are able to confine most of the light into the core thus making it highly sensitive and reliable. The values for confinement loss are 1.48E-14 dB/m for decagonal at 1.33μm wavelength.[30], [20]

Chapter 6

Comparative study and results of various structures filled with different materials

6.1 Effective refractive index Vs Wavelength

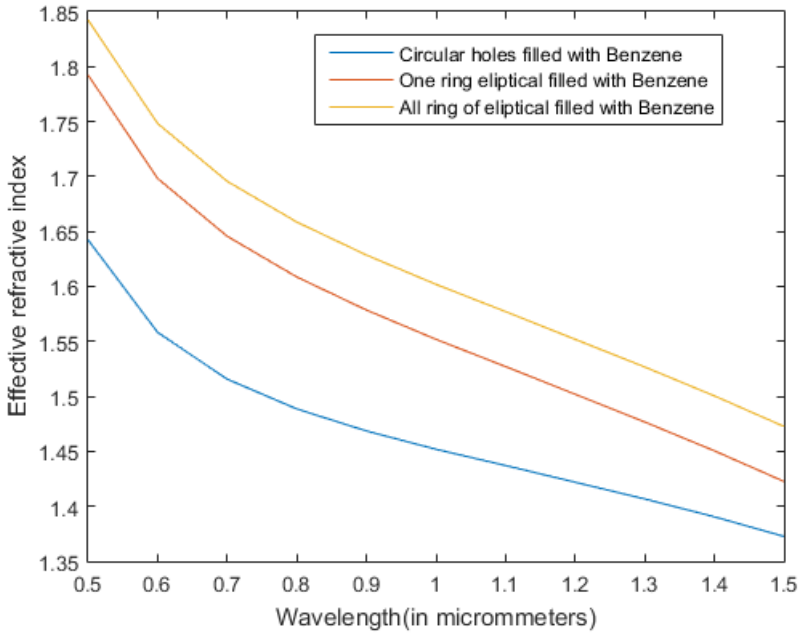

Figure 6.1: Effective refractive index Vs Wavelength for Benzene

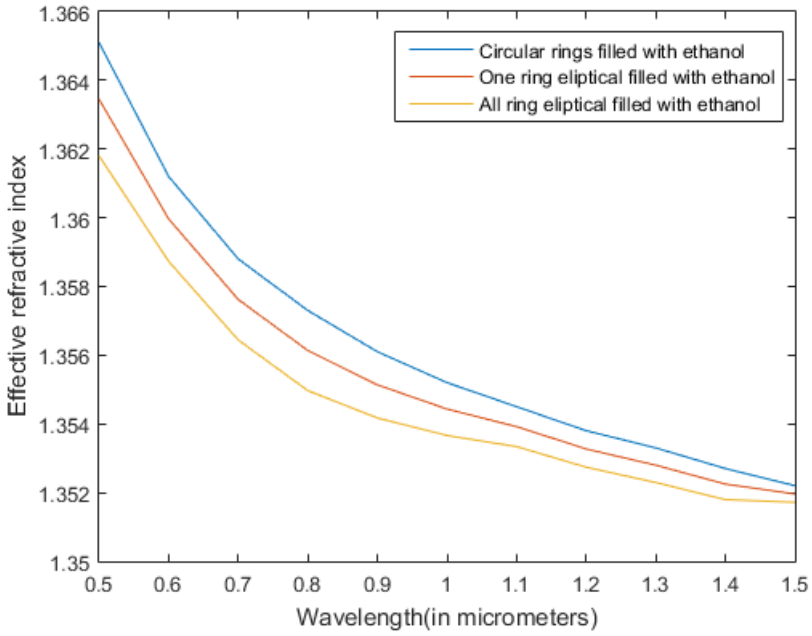

Figure 6.2: Effective refractive index Vs Wavelength for Ethanol

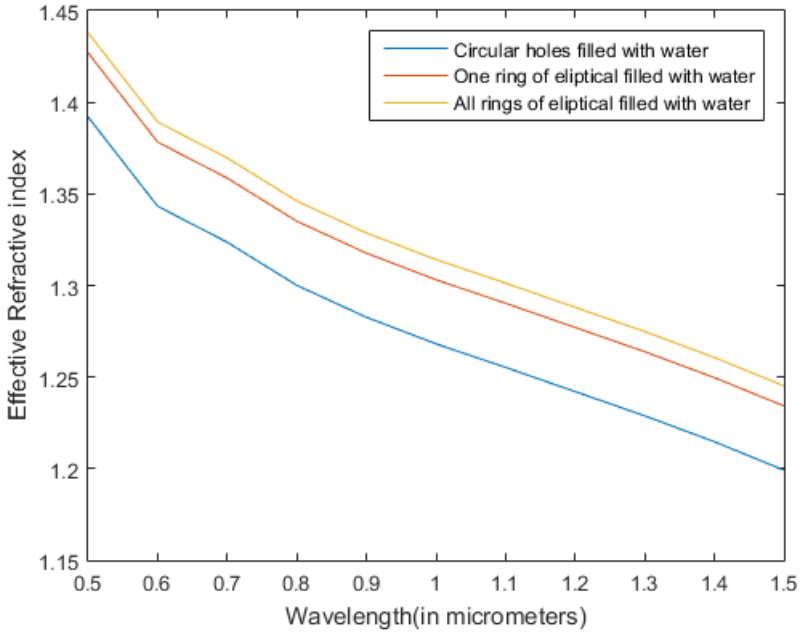

Figure 6.3: Effective refractive index Vs Wavelength for Water

6.1. Effective refractive index Vs Wavelength

Wavelength(μm)	Benzene	Ethanol	Water
0.5	1.5053	1.3651	1.3350
0.6	1.4948	1.3612	1.3321
0.7	1.4889	1.3588	1.3311
0.8	1.4853	1.3573	1.3290
0.9	1.4828	1.3561	1.3281
0.1	1.4810	1.3552	1.3272
1.1	1.4798	1.3545	1.3255
1.3	1.4781	1.3533	1.32225
1.4	1.4775	1.3527	1.3213
1.5	1.4770	1.3522	1.3190

Table 6.1: Table Showing Refractive index variation with wavelength for Benzene Ethanol and Water

Effective refractive index is decreasing with wavelength according to the Sellemeier's equation which states that η_{eff} is inversely proportional to wavelength. It has higher value for denser medium as can be seen from the graph. The values of η_{eff} at $1.33\mu m$ wavelength are 1.375, 1.329 and 1.321 for Benzene, Ethanol and Water respectively.

6.2 Confinement loss vs Wavelength

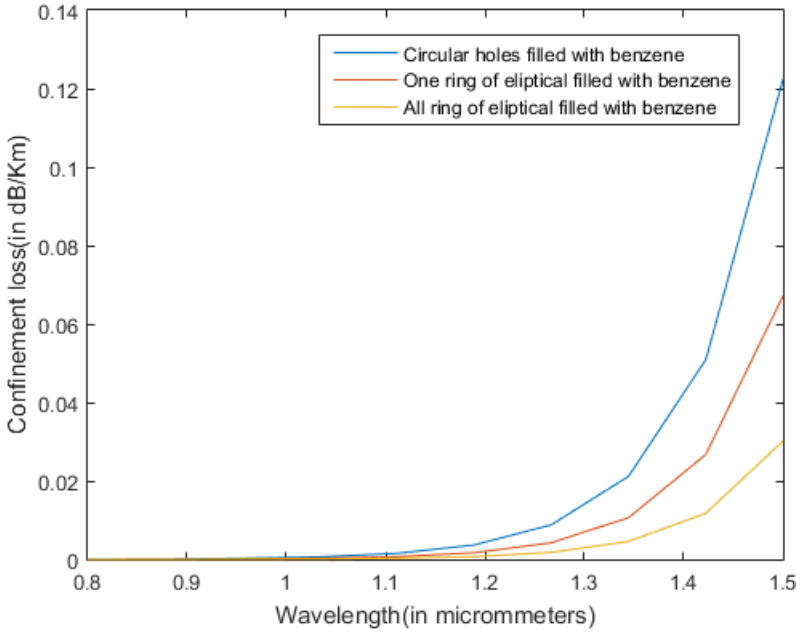

Figure 6.4: Confinement loss Vs Wavelength for Benzene

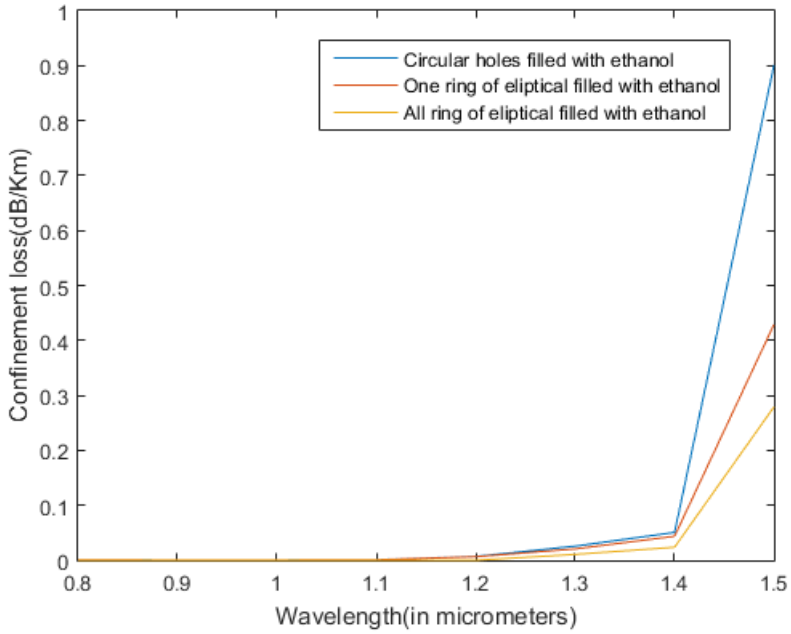

Figure 6.5: Confinement loss Vs Wavelength for Ethanol

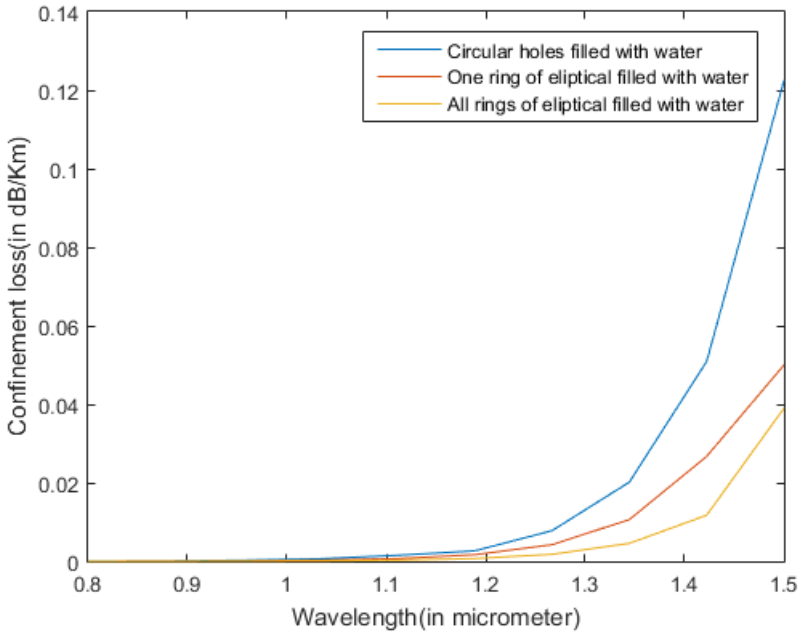

Figure 6.6: Confinement loss Vs Wavelength for Water

Wavelength(μm)	Benzene	Ethanol	Water
0.8	mode not found	0.000681851	0.000681040
0.9	mode not found	0.00060609	0.00060508
1.0	0.000545481	0.000545481	0.000505081
1.1	0.002479458	0.000991783	0.000801782
1.2	0.009091347	0.007273077	0.006261075
1.3	0.029372043	0.027693641	0.020693451
1.4	0.057665113	0.055716967	0.050715437
1.5	0.097459236	0.094913659	0.090803054

Table 6.2: Table Showing Confinement loss with wavelength for Benzene Ethanol and Water

The confinement loss as seen from the graph is almost negligible, which states that the geometry used are able to confine most of the light into the core thus making it highly sensitive and reliable. The minimum value of confinement loss is obtained from

the structure where all the layers are taken of elliptical shape of holes and value of confinement loss comes to 0.09745(dB/Km).

6.3 Dispersion Vs Wavelength

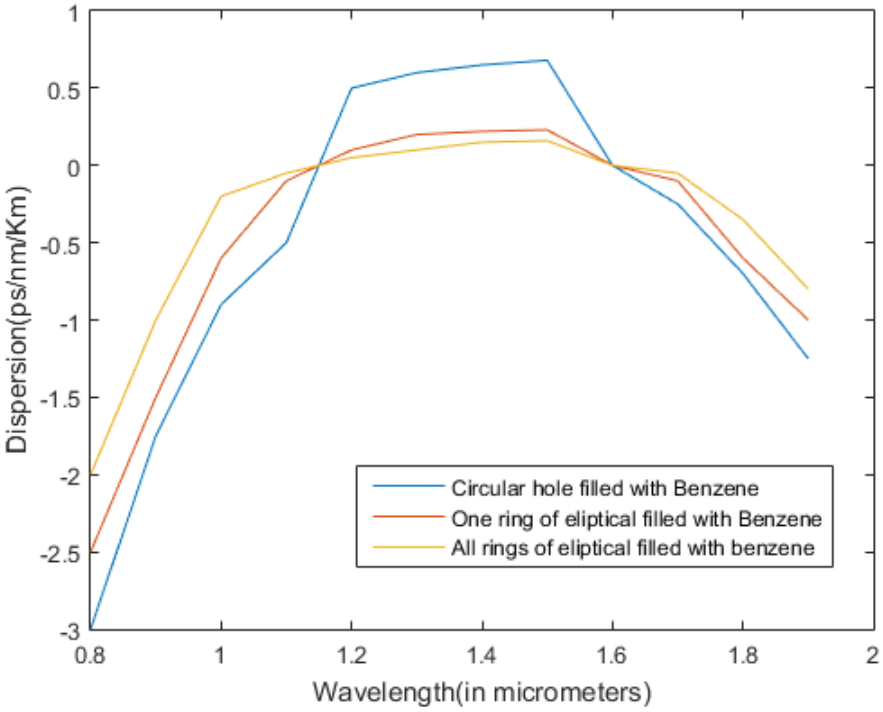

Figure 6.7: Confinement loss Vs Wavelength for Benzene

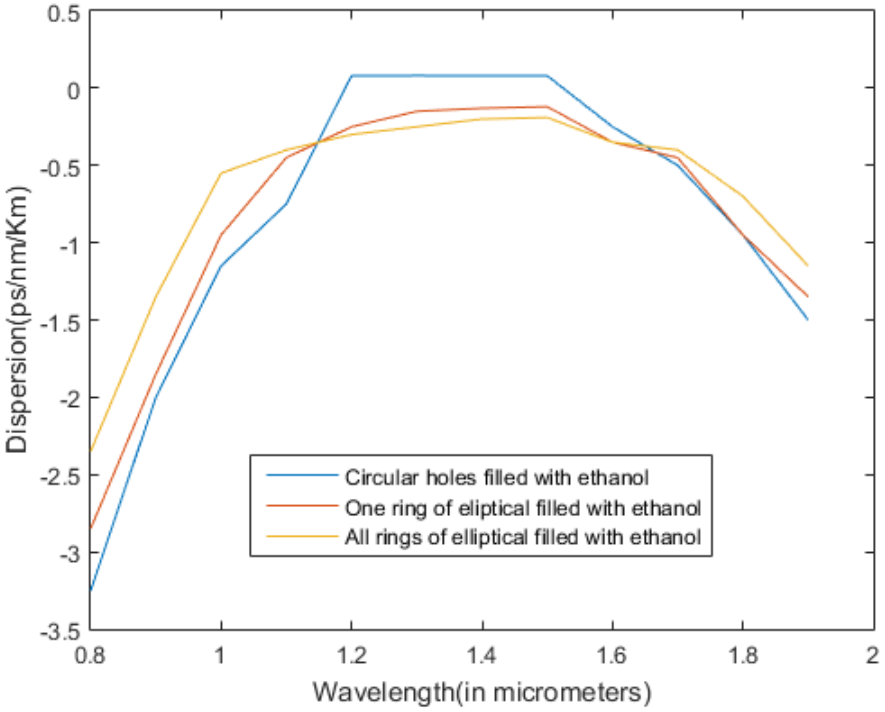

Figure 6.8: Confinement loss Vs Wavelength for Ethanol

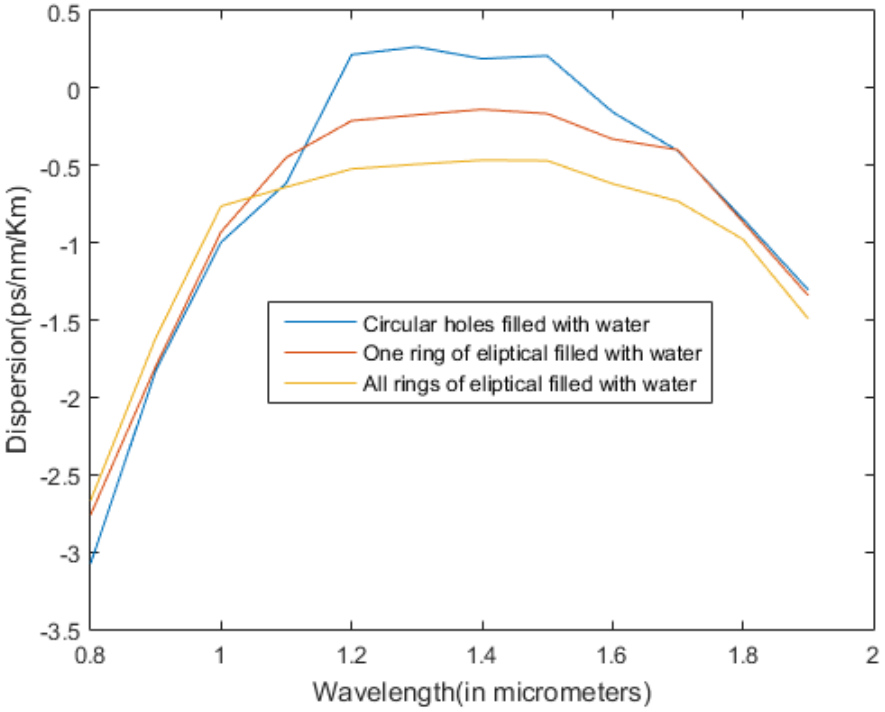

Figure 6.9: Confinement loss Vs Wavelength for Water

Wavelength(μm)	Benzene	Ethanol	Water
0.8	-3.000	-2.7500	-2.00
0.9	-1.750	-1.500	-1.00
1.0	-0.900	-0.600	-0.20
1.1	-0.500	-0.100	-0.050
1.2	0.50	0.100	0.0050
1.3	0.600	0.200	0.100
1.4	0.650	0.220	0.150
1.5	0.68	0.230	0.16
1.6	0.00	0.00	0.00
1.7	-0.25	-0.100	-0.05
1.8	-0.70	-0.60	-0.35
1.9	-1.250	-1.00	-0.800

Table 6.3: Table Showing Dispersion with wavelength for Benzene Ethanol and Water

In photonic crystal fiber the total dispersion is the sum of material dispersion and the waveguide dispersion. Based on the simulation results it is conluded that the value of dispersion is increasing with wavelength but after a particular wavelength(zero-dispersion wavelength) the value of dispersion becomes zero. From the results the value of this wavelength is found to be $1.65\mu m$ for the structure where all the rings are of elliptical holes.

References

[1] A. Rifat, G. Mahdiraji, D. Chow, Y. Shee, R. Ahmed, and F. Adikan, "Photonic crystal fiber-based surface plasmon resonance sensor with selective analyte channels and graphene-silver deposited core," *Sensors*, vol. 15, no. 5, pp. 11499–11510, 2015.

[2] K. Saitoh, M. Koshiba, T. Hasegawa, and E. Sasaoka, "Chromatic dispersion control in photonic crystal fibers: application to ultra-flattened dispersion," *Optics Express*, vol. 11, no. 8, pp. 843–852, 2003.

[3] G. Keiser, "Optical fiber communications," *Wiley Encyclopedia of Telecommunications*, 2003.

[4] J. Knight, T. Birks, P. S. J. Russell, and D. Atkin, "All-silica single-mode optical fiber with photonic crystal cladding," *Optics letters*, vol. 21, no. 19, pp. 1547–1549, 1996.

[5] J. Xue, S. Li, Y. Xiao, W. Qin, X. Xin, and X. Zhu, "Polarization filter characters of the gold-coated and the liquid filled photonic crystal fiber based on surface plasmon resonance," *Optics express*, vol. 21, no. 11, pp. 13733–13740, 2013.

[6] Y. Zhao, Z.-q. Deng, and J. Li, "Photonic crystal fiber based surface plasmon resonance chemical sensors," *Sensors and Actuators B: Chemical*, vol. 202, pp. 557–567, 2014.

[7] M. Li, L. Peng, G. Zhou, B. Li, Z. Hou, and C. Xia, "Design of photonic crystal fiber filter with narrow width and single-polarization based on surface plasmon resonance," *IEEE Photonics Journal*, vol. 9, no. 3, pp. 1–8, 2017.

[8] H. Li, S. Li, H. Chen, J. Li, G. An, and J. Zi, "A polarization filter based on photonic crystal fiber with asymmetry around gold-coated holes," *Plasmonics*, vol. 11, no. 1, pp. 103–108, 2016.

[9] S. A. Cerqueira Jr, "Recent progress and novel applications of photonic crystal fibers," *Reports on progress in physics*, vol. 73, no. 2, p. 024401, 2010.

[10] J. C. Knight, "Photonic crystal fibres," *nature*, vol. 424, no. 6950, p. 847, 2003.

[11] D. Chen and L. Shen, "Ultrahigh birefringent photonic crystal fiber with ultralow confinement loss," *IEEE Photonics Technology Letters*, vol. 19, no. 4, pp. 185–187, 2007.

[12] Y. Wang, N. V. Wheeler, F. Couny, P. Roberts, and F. Benabid, "Low loss broadband transmission in hypocycloid-core kagome hollow-core photonic crystal fiber," *Optics letters*, vol. 36, no. 5, pp. 669–671, 2011.

[13] B. Dabas and R. Sinha, "Dispersion characteristic of hexagonal and square lattice chalcogenide as2se3 glass photonic crystal fiber," *Optics Communications*, vol. 283, no. 7, pp. 1331–1337, 2010.

[14] M. F. O. Hameed, A. Heikal, B. Younis, M. Abdelrazzak, and S. Obayya, "Ultra-high tunable liquid crystal-plasmonic photonic crystal fiber polarization filter," *Optics express*, vol. 23, no. 6, pp. 7007–7020, 2015.

[15] M. Koshiba and K. Saitoh, "Numerical verification of degeneracy in hexagonal photonic crystal fibers," *IEEE Photonics Technology Letters*, vol. 13, no. 12, pp. 1313–1315, 2001.

[16] T. A. Birks, J. C. Knight, and P. S. J. Russell, "Endlessly single-mode photonic crystal fiber," *Optics letters*, vol. 22, no. 13, pp. 961–963, 1997.

[17] R. Sinha and S. K. Varshney, "Dispersion properties of photonic crystal fibers," *Microwave and optical technology letters*, vol. 37, no. 2, pp. 129–132, 2003.

[18] A. Yariv, *Optical electronics*. Saunders College Publ., 1991.

[19] V. Bhatia and A. M. Vengsarkar, "Optical fiber long-period grating sensors," *Optics letters*, vol. 21, no. 9, pp. 692–694, 1996.

[20] A. Hochman and Y. Leviatan, "Calculation of confinement losses in photonic crystal fibers by use of a source-model technique," *JOSA B*, vol. 22, no. 2, pp. 474–480, 2005.

[21] F. Bréchet, J. Marcou, D. Pagnoux, and P. Roy, "Complete analysis of the characteristics of propagation into photonic crystal fibers, by the finite element method," *Optical Fiber Technology*, vol. 6, no. 2, pp. 181–191, 2000.

[22] A. Ferrando, E. Silvestre, P. Andrés, J. J. Miret, and M. V. Andrés, "Designing the properties of dispersion-flattened photonic crystal fibers," *Optics Express*, vol. 9, no. 13, pp. 687–697, 2001.

[23] M. Steel and R. Osgood, "Polarization and dispersive properties of elliptical-hole photonic crystal fibers," *Journal of Lightwave Technology*, vol. 19, no. 4, p. 495, 2001.

[24] A. Bjarklev, J. Broeng, K. Dridi, and S. E. Barkou, "Dispersion properties of photonic crystal fibres," in *24th European Conference on Optical Communication. ECOC'98 (IEEE Cat. No. 98TH8398)*, vol. 1, pp. 135–136, IEEE, 1998.

[25] J. Knight, J. Arriaga, T. Birks, A. Ortigosa-Blanch, W. Wadsworth, and P. S. J. Russell, "Anomalous dispersion in photonic crystal fiber," *IEEE photonics technology letters*, vol. 12, no. 7, pp. 807–809, 2000.

[26] K. M. Hilligsøe, T. V. Andersen, H. N. Paulsen, C. K. Nielsen, K. Mølmer, S. Keiding, R. Kristiansen, K. P. Hansen, and J. J. Larsen, "Supercontinuum generation in a photonic crystal fiber with two zero dispersion wavelengths," *Optics Express*, vol. 12, no. 6, pp. 1045–1054, 2004.

[27] W. H. Reeves, J. Knight, P. S. J. Russell, and P. Roberts, "Demonstration of ultra-flattened dispersion in photonic crystal fibers," *Optics express*, vol. 10, no. 14, pp. 609–613, 2002.

[28] K. P. Hansen, "Dispersion flattened hybrid-core nonlinear photonic crystal fiber," *Optics Express*, vol. 11, no. 13, pp. 1503–1509, 2003.

[29] T. Matsui, J. Zhou, K. Nakajima, and I. Sankawa, "Dispersion-flattened photonic crystal fiber with large effective area and low confinement loss," *Journal of Lightwave Technology*, vol. 23, no. 12, pp. 4178–4183, 2005.

[30] A. Argyros, I. M. Bassett, M. A. Van Eijkelenborg, M. C. Large, J. Zagari, N. A. Nicorovici, R. C. McPhedran, and C. M. de Sterke, "Ring structures in microstructured polymer optical fibres," *Optics Express*, vol. 9, no. 13, pp. 813–820, 2001.